



**WATER PARTICLE DISPERSION  
IN A  
TURBULENT VERTICAL AIR FLOW**

by

Timothy K. Wheeler

---

Thesis  
for the  
Degree of Bachelor of Science  
in  
Chemical Engineering

College of Liberal Arts and Sciences  
University of Illinois  
Urbana, Illinois

1992

## **WATER PARTICLE DISPERSION IN A TURBULENT VERTICAL AIR FLOW**

**Timothy K. Wheeler  
Department of Chemical Engineering  
University of Illinois at Urbana-Champaign, 1992  
Professor Thomas J. Hanratty**

The motion of water particles injected into the center of a turbulent pipe flow was studied in this investigation. The results were used to analyze the correlation developed by Lee that relates the turbulent intensities of the particles and fluid to the inverse inertial time constant of the particles and the Lagrangian integral time scale of the fluid. The data acquired in this investigation was also used to predict the fraction of droplets deposited on the pipe wall as a function of time based on Lee's particle deposition model.

The particles studied were 150  $\mu\text{m}$  in diameter. They were injected into a vertical air flow exhibiting a Reynolds number of 52,000 at a point 114 cm above where the data was taken. Photographs of the droplet images were analyzed using an image processing system to determine the coordinates necessary to calculate the velocities and concentrations of the droplets.

It was found that the eddy diffusivity of the particles was 15.19  $\text{cm}^2/\text{s}$ . The ratio of the eddy diffusivity of the particles to the eddy diffusivity of the fluid was 0.963. The measured root turbulent radial intensity of the particles was found to be 19.57  $\text{cm/s}$  and the root particle to fluid intensity ratio was calculated as 0.357. This value was compared to a theoretical value calculated using equation 2.6 to evaluate the accuracy of the correlation developed by Lee. The theoretical value was found to be 0.344 showing the correlation accurately predicts the ratio of the particle to fluid intensities.

## **ACKNOWLEDGMENT**

**I would like to express my thanks to Dr. Thomas J. Hanratty for all his help and patience and for giving me the opportunity to work on this project.**

**The help of Dr. Liu and James Hay was also greatly appreciated.**

**I would also like to thank John Bilardello, John Schumacher, Nader Ameli, Roger and Nurse Siemens, Suz Wheeler, Kim Fette, Lysh, my parents, Bolo Yung, Mike George, Barry Baldwin, Clive Peers, the rest of the Bilardellos, Bob Springer, Bill Nelson, Tamrat, Bagel, Kelly Sowa and even Heidi .**

**Special thanks to Mark Sowa and Prince.**

## TABLE OF CONTENTS

<b>I. Introduction .....</b>	<b>1</b>
<b>II. Theory .....</b>	<b>2</b>
A.) Review of Lee's Deposition Model .....	2
B.) Turbulent Intensities .....	3
C.) Eddy Diffusivities .....	6
<b>III. Experimental .....</b>	<b>7</b>
A.) Flow System .....	7
B.) Injection System .....	7
C.) Optical System .....	12
D.) Experimental Procedure .....	15
E.) Film Developing .....	16
F.) Image Processing .....	16
<b>IV. Results .....</b>	<b>18</b>
A.) Droplet Concentrations .....	18
B.) Droplet Velocities .....	18
C.) Eddy Diffusivities .....	23
D.) Velocity Analysis .....	23
<b>V. Discussion .....</b>	<b>27</b>
A.) Velocity Measurements .....	27
B.) Particle Deposition .....	29
<b>Computer Programs .....</b>	<b>Appendix A</b>
<b>Calibration Charts .....</b>	<b>Appendix B</b>

## LIST OF SYMBOLS

$C$	particle number concentration
$C_d$	drag coefficient of the particles
$d_j$	injector water jet diameter
$d_p$	particle diameter
$d_t$	pipe (tube) diameter
$f$	Fanning friction factor
$g$	gravitational constant
$J_0, J_1$	Bessel functions
$k$	constant defined by equation 2.16
$N$	total number of particles
$Q$	water flow rate to the injector
$R$	pipe radius
$r$	radial distance from the pipe center
$r'$	radial injection point of the particles
$Re_f$	fluid Reynolds number
$Re_p$	particle Reynolds number
$t$	time
$U_f$	mean axial fluid velocity
$U_t$	particle terminal velocity
$u^*$	friction velocity of the fluid
$V$	volume of a concentration sector
$v_r$	particle radial velocity
$v_\theta$	particle tangential velocity
$\overline{x_p^2}$	mean square droplet displacement
$z$	axial distance of particles downstream from the injector tip

### Greek Symbols

$\alpha_n$	Fourier constants
$\beta$	inverse inertial time constant of the particles
$\epsilon_p$	particle eddy diffusivity
$\epsilon_f$	fluid eddy diffusivity
$\mu_f$	fluid viscosity
$\rho_f$	fluid density
$\rho_p$	particle density
$\tau_f$	Lagrangian integral time scale of the fluid
$\overline{u_{f,r}^2}$	fluid mean square radial turbulent fluctuation (intensity)
$\overline{u_r^2}$	particle mean square radial turbulent fluctuation (intensity)
$\overline{u_\theta^2}$	particle mean square tangential turbulent fluctuation (intensity)

- a bar over any symbol indicates a mean value

## INTRODUCTION

A critical issue in understanding annular gas liquid flows is the prediction of the fraction of the liquid entrained in the gas as droplets. The prediction of this entrainment requires a knowledge of the turbulence properties or the droplets. Lee [3] developed a diffusion model to predict droplet concentration and deposition for drops ranging from  $20\mu\text{m}$  to  $200\mu\text{m}$  in diameter. Lee also developed a correlation relating the average droplet turbulent intensity to that of the fluid.

This research tests the correlations proposed by Lee with turbulence measurements of  $150\mu\text{m}$  droplets in a vertical turbulent air flow exhibiting a Reynolds number of 52,000. An optical detection technique is used to obtain a photograph of the droplets in a horizontal plane. This technique allows several images of each droplet to be captured. The photographs can be analyzed using image processing equipment to determine the coordinates of each image. From the distance and time between each successive image it is possible to determine a droplet's velocity. The droplet coordinates can also be used to determine the droplet concentration profile. From the concentrations and velocities measured, the particle eddy diffusivities and turbulent intensities can be calculated.

The particle deposition model developed by Lee requires the particle eddy diffusivity and the particle intensity within one stopping distance from the wall to calculate the fraction of particles deposited at the pipe wall at a given time. It is possible to calculate both of these from the type of measurements presented in this thesis.

Lee developed related the root mean square radial velocity fluctuations of the particles to the turbulent fluctuation of the fluid and to the ratio of the inertial time constant of the particles and the Lagrangian integral time scale of the fluid. The testing of the accuracy of this correlation is the main focus of this research.



## II. THEORY

### A. Review of Lee's Deposition Model

The deposition model developed by Michael Lee [3] gives an estimation of the fraction of water particles originated from a point source to deposit on the pipe wall at a given time. It is based on a random walk assumption and therefore uses the standard diffusion equation

$$\epsilon_p \nabla^2 C(r,t) = \frac{\partial C(r,t)}{\partial t} \quad (2.1)$$

where  $\epsilon_p$  is the diffusion coefficient of the particles and  $C(r,t)$  is the number concentration of the particles at radial position  $r$  and time  $t$ . A plug flow is assured so that  $t = z/U_f$ . Lee derived the boundary condition at  $r=R$  for equation 2.1 as

$$-\epsilon_p \frac{\partial C(r,t)}{\partial r} \bigg|_{r=R} = \sqrt{\frac{1}{2\pi}} (\overline{v_r^2})^{1/2} C(r,t) \bigg|_{r=R} \quad (2.2)$$

where  $(\overline{v_r^2})^{1/2}$  is the root mean square of the radial velocity of the particles. Solving equation 2.1 applying boundary condition 2.2 gives

$$C(r,t) = \frac{N}{U_f \pi R^2} \sum_{n=1}^{\infty} e^{-\epsilon_p \alpha_n^2 t} \frac{J_0(r \alpha_n) J_0(r' \alpha_n)}{J_0^2(R \alpha_n) + J_1^2(R \alpha_n)} \quad (2.3)$$

where  $N$  is the total number of particles injected per unit time,  $U_f$  is the mean velocity of the fluid,  $r'$  is the radial location where the particles are injected,  $\alpha_n$  are positive Fourier coefficients, and  $J_0$  and  $J_1$  are Bessel functions. Assuming  $r'$  to be zero as the particles are injected at the center of the pipe, equation 2.3 was shown by Lee to yield the relationship

$$\text{fraction deposited (at time } t) = \frac{2}{R} \sum_{n=1}^{\infty} \frac{J_1(R \alpha_n)}{\alpha_n (J_0^2(R \alpha_n) + J_1^2(R \alpha_n))} (e^{-\epsilon_p \alpha_n^2 t_0} - e^{-\epsilon_p \alpha_n^2 t}) \quad (2.4)$$

where the Fourier coefficients are given by

$$\alpha_{n+1} = \alpha_n - \frac{\epsilon_p \alpha_n J_1(R\alpha_n) - (1/\sqrt{2\pi}) (\overline{v_r^2})^{1/2} J_0(R\alpha_n)}{\epsilon_p R \alpha_n J_0(R\alpha_n) + R (\overline{v_r^2})^{1/2} J_1(R\alpha_n)} \quad (2.5)$$

Lee's model therefore contains only two parameters: the root mean squared turbulent fluctuation and the eddy diffusivity of the particles both of which could be determined experimentally by the methods in the discussion that follows. The computer program written by Lee shown in Appendix A solves the deposition model.

### B. Turbulent Intensities

Lee also developed a correlation for droplet turbulent intensity [3]. He found that

$$\frac{(\overline{v_r^2})^{1/2}}{(\overline{v_{f,r}^2})^{1/2}} = \left( \frac{\beta \tau_f}{0.7 + \beta \tau_f} \right)^{1/2} \quad (2.6)$$

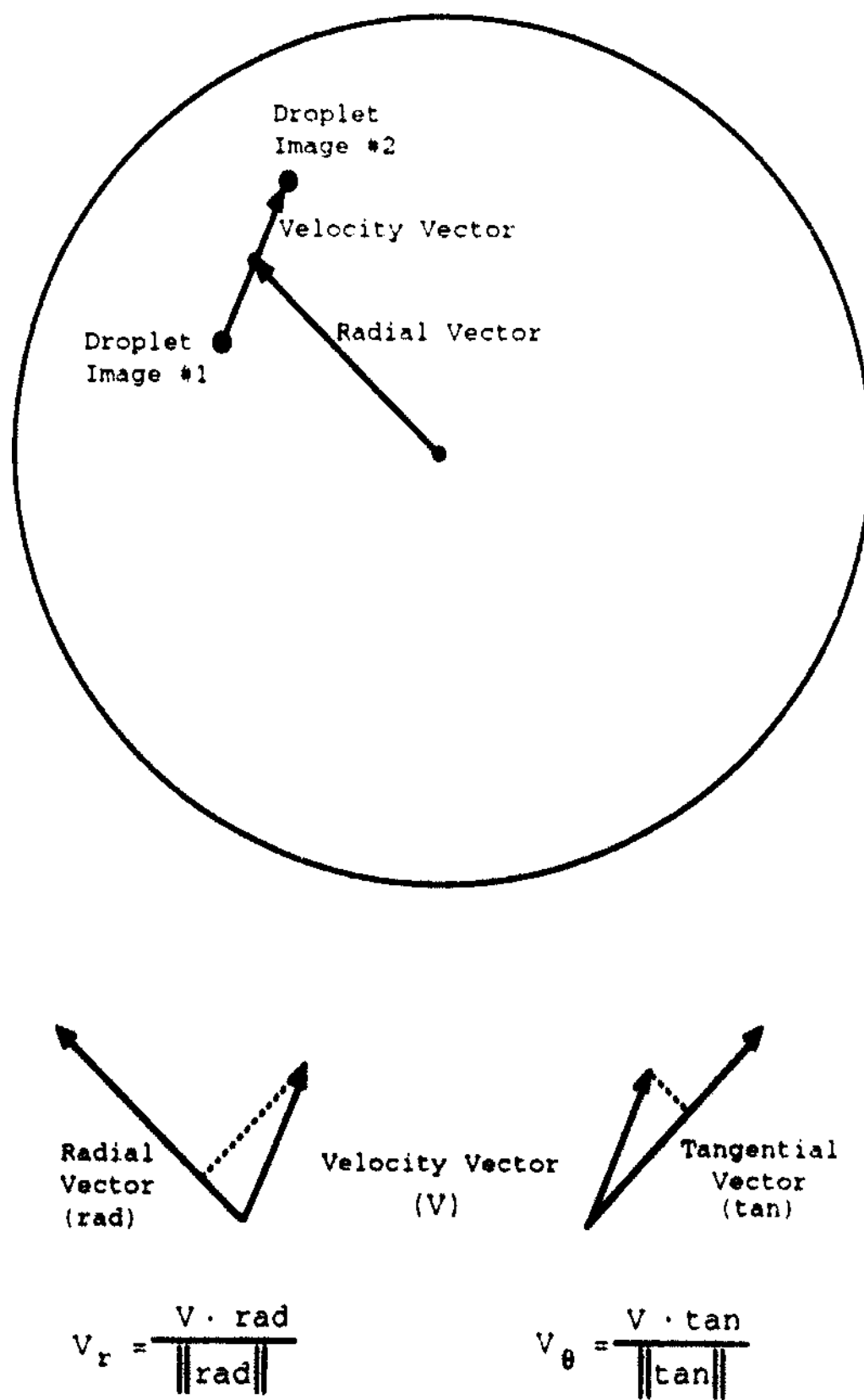
where  $\overline{v_{f,r}^2}$  is the mean square turbulent fluctuation of the fluid in the radial direction,  $\beta$  is the inverse inertial time constant of the particles, and  $\tau_f$  is the Lagrangian integral time scale of the fluid which is a measure of the average turbulent eddy lifetime. The constant, 0.7, is value Lee found from a best fit to his data. According to Vames [6], the turbulent fluctuation of the fluid is

$$\overline{v_{f,r}^2} = (0.19 U_f \text{Re}_f^{-1/6})^2 \quad (2.7)$$

where  $U_f$  is the mean axial velocity of the fluid and  $\text{Re}_f$  is the Reynolds number of the fluid.

The mean square radial fluctuation of the particles is found from the experimental data. A drawing of a typical photograph is shown in figure 2.1. The velocity vector of the particle is found by subtracting the position of the second image from the position of the first image. The tangential and radial components are given by the projection of the velocity vector on to the radial or tangential vector using the equations shown in figure 2.1. The radial vector is found by subtracting the coordinates of the center of the pipe from the coordinates of the midpoint between the two images. Exchanging the i and j

Figure 2.1: Velocity Calculation



value of the radial vector and changing the sign of the  $i$  value gives the tangential vector. The mean radial velocity and the mean square radial velocity can be calculated from

$$\overline{v_r} = \frac{1}{n} \sum_{i=1}^n v_{r,i} \quad \overline{v_r^2} = \frac{1}{n} \sum_{i=1}^n v_{r,i}^2 \quad (2.8)$$

The turbulent intensity,  $\overline{v_r^2}$ , is then found from the difference between the mean square radial velocity and the square of the mean radial velocity.

The inverse inertial time constant can be determined by the following equation according to Lee

$$\beta = \frac{3 C_d \rho_f U_t}{4 d_p \rho_p} \quad (2.9)$$

where  $C_d$  is the drag coefficient of the particle,  $\rho_p$  and  $\rho_f$  are the densities of the fluid and the particle,  $U_t$  is the terminal velocity of the particle, and  $d_p$  is the particle diameter. The drag coefficient for a sphere can be found in Bennett and Myers [1] from the Reynolds number of the particle given by

$$Re_f = \rho_f U_t d_p / \mu_f \quad (2.10)$$

where  $\mu_f$  is the viscosity of the fluid. The terminal velocity of the particle is determined using Stoke's law [4].

$$U_t = g d_p^2 (\rho_p - \rho_f) / \mu_f \quad (2.11)$$

The Lagrangian integral time scale of the fluid,  $\tau_f$ , is calculated from the equation [3]

$$\tau_f = \frac{\epsilon_f}{\overline{v_f^2}} \quad (2.12)$$

The eddy diffusivity of the fluid,  $\epsilon_f$ , is given by the equation

$$\epsilon_f = (0.037) d_t u^* \quad (2.13)$$

according to Vames [6]. The term  $u^*$  is the friction velocity of the fluid determined from the Blasius equation

$$u^* = U_f (f / 2)^{1/2} \quad (2.14)$$

where the Fanning friction factor,  $f$ , is given by [6]

$$f = (.00791) \text{Re}_f^{1/4}$$

(2.15) 6

### C. Eddy Diffusivities

Measurements of the radial velocity at given distances from the center of the pipe can be reasonably well fitted with a straight line to yield the equation [7]

$$v_r = k r \quad (2.16)$$

where  $v_r$  is the average particle velocity at radial distance,  $r$ . The fluid eddy diffusivity can be found from

$$\epsilon_p = N(r) / \left( - \frac{dC}{dr} \right) \quad (2.17)$$

The concentration profile can be fitted with a Gaussian distribution and the number of particles at  $r$ ,  $N(r)$ , is equal to the particle concentration at  $r$  multiplied by the velocity at  $r$ . Therefore, according to Young [7], the eddy diffusivity of the particles can be calculated from the equation

$$\epsilon_p = k \overline{X_p^2} \quad (2.18)$$

$\overline{X_p^2}$  is the mean squared droplet displacement and the constant  $k$  is defined in equation 2.16. The droplet displacement is determined from the Gaussian distribution

$$\ln C = \frac{-1}{2 \overline{X_p^2}} r^2 + b \quad (2.19)$$

where  $C$  is the number concentration of particles,  $r$  is the radial distance from the center of the pipe, and  $b$  is a constant.

### III. EXPERIMENTAL

#### A. Flow System

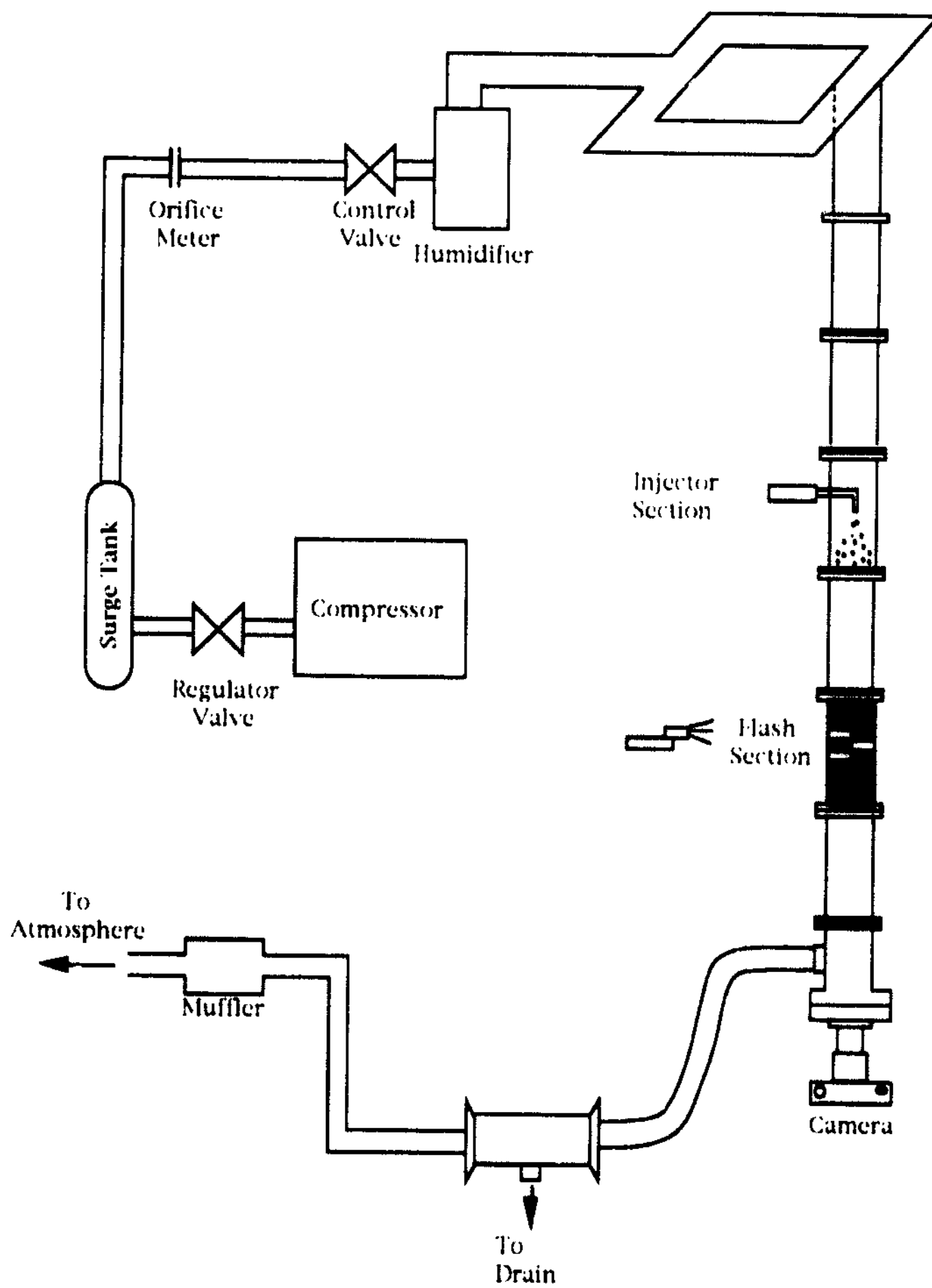
The flow system developed by Vames and Lee was used in this research. The schematic diagram of the system is shown in figure 3.1. Air flowed downward in a vertical pipe. It was supplied by an Ingersoll-Rand air compressor that could deliver 220 std. ft<sup>3</sup> / min. with an outlet pressure of 110 psig. Upon exiting the compressor, the air passed through a filter and a 100 gallon surge tank to create a clean, steady air flow. The flow rate through the system was controlled by a differential pressure controller. An orifice meter with a hole size of 0.262 inch was used to find the pressure drop along the one inch line leading to the test section. The orifice coefficients were given by a graph taken from Lee (1987), which can be found in appendix B. A computer program written by Lee was used to calculate the velocity and Reynolds number of the air flow. The program is printed out in appendix A. A humidifier was added to the system to prevent excessive particle evaporation. A tee section before the test section created a fully turbulent flow.

The vertical test section of the system consists of several sections of 2 inch inner diameter piping, primarily made of brass or PVC. The injector section is made of plexiglass and located at least 60 pipe diameters below the tee section. It could be moved to give a range of distances between the injection point and the flash section. Both the flash section and the camera port are also constructed of plexiglass. A separator follows the test section to remove any water particles remaining in the air. The exhaust discharges to the atmosphere through a muffler.

#### B. Injection System

The droplet injection system developed by Vames (1987) was used for this investigation. It is shown in figure 3.2. It consists of a pressurized water reservoir that supplies water to the injector. The flow rate is controlled with a regulator valve and measured using a Gilmont rotameter; the calibration curve is shown in appendix B. A Sybron/Barnstead Nanopure system provides the water for the reservoir. Several filters are located before the

Figure 3.1: Flow System



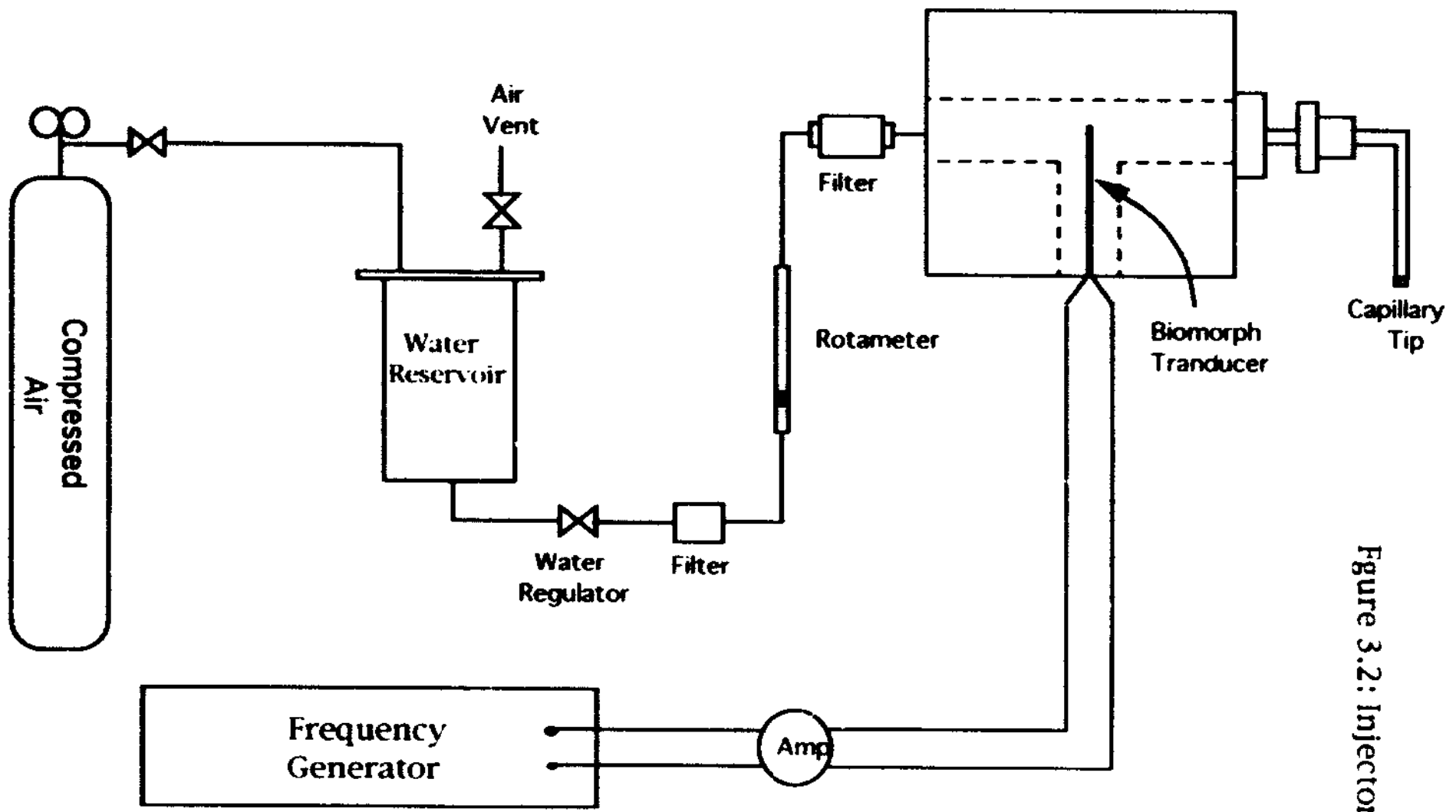


Figure 3.2: Injector System



to prevent clogging or deflection of the stream.

10

The injector consists of a plexiglass droplet generation chamber, a stainless steel tube, and a thin piece of glass capillary tubing. Vibrations created in the droplet generation chamber by a biomorph transducer are transmitted through the steel tube to the capillary tip where they cause the water stream to separate into uniform droplets. The frequency of the vibrations used depended on the particle size and the air velocity. The volumetric flow rate was chosen so the velocity of the particle stream exiting the injector tip was equal to the velocity of the air flowing through the test section. The volumetric flow rate was calculated from

$$Q = U_f \pi d_j^2 / 4$$

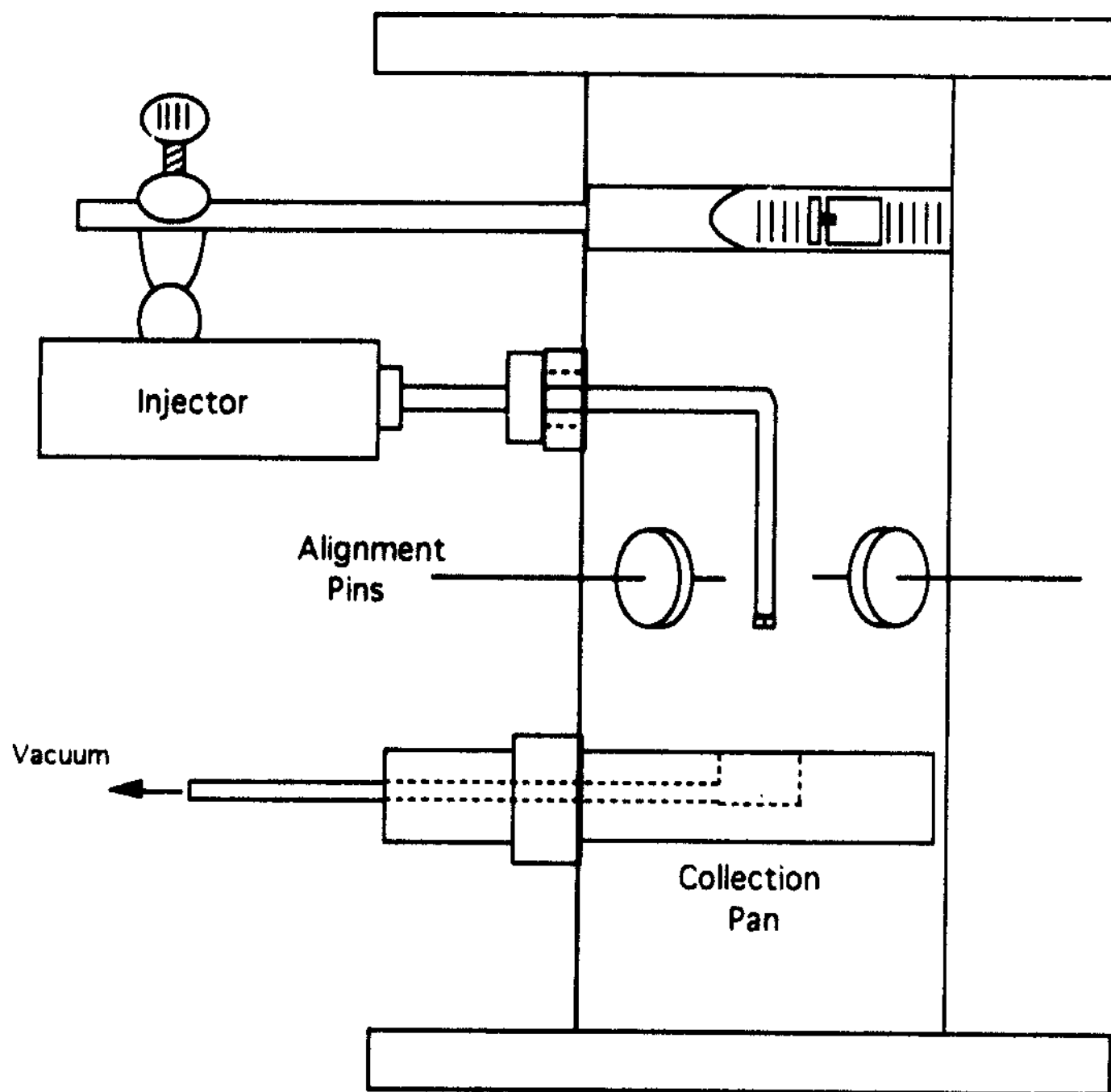
The biomorph transducer is controlled by a Wavetek function generator with a maximum output of 20 volts peak to peak. It is necessary to amplify this signal to 70 volts peak to peak to produce the desired effect. The frequency of the sine wave generated was determined by

$$f = \frac{6Q}{d_p^3 \pi}$$

The injector tip is changed to produce different sized droplets by the following procedure: First, one end of a glass capillary tube of the desired bore size is sanded and polished. The capillary is then scored and broken off about 0.5 cm from the end. The smooth end is adhered to the steel tube using Loctite Ultraviolet Curing Glass Adhesive and a 4 watt UV lamp. The exposed glass end is ground down to a width of only one millimeter so as to have a small pressure drop. The injector is then tested using a strobe light to check the uniformity of the droplets and the trajectory of the stream of drops.

A plexiglass segment of the test section was specially designed to house the injector. It is shown in figure 3.3. The injector is inserted through a half-inch circular opening in the side of the tube and held in place by means of a clamp and a plug along the steel tube. Four thin steel rods are used to properly align the injector once it is in place. A collection pan attached to a vacuum line is located below the injector tip to collect the water when the system is not being used. Both the steel alignment rods and the collection pan are pulled out until flush with the wall during experiments.

Figure 3.3: Injector Section



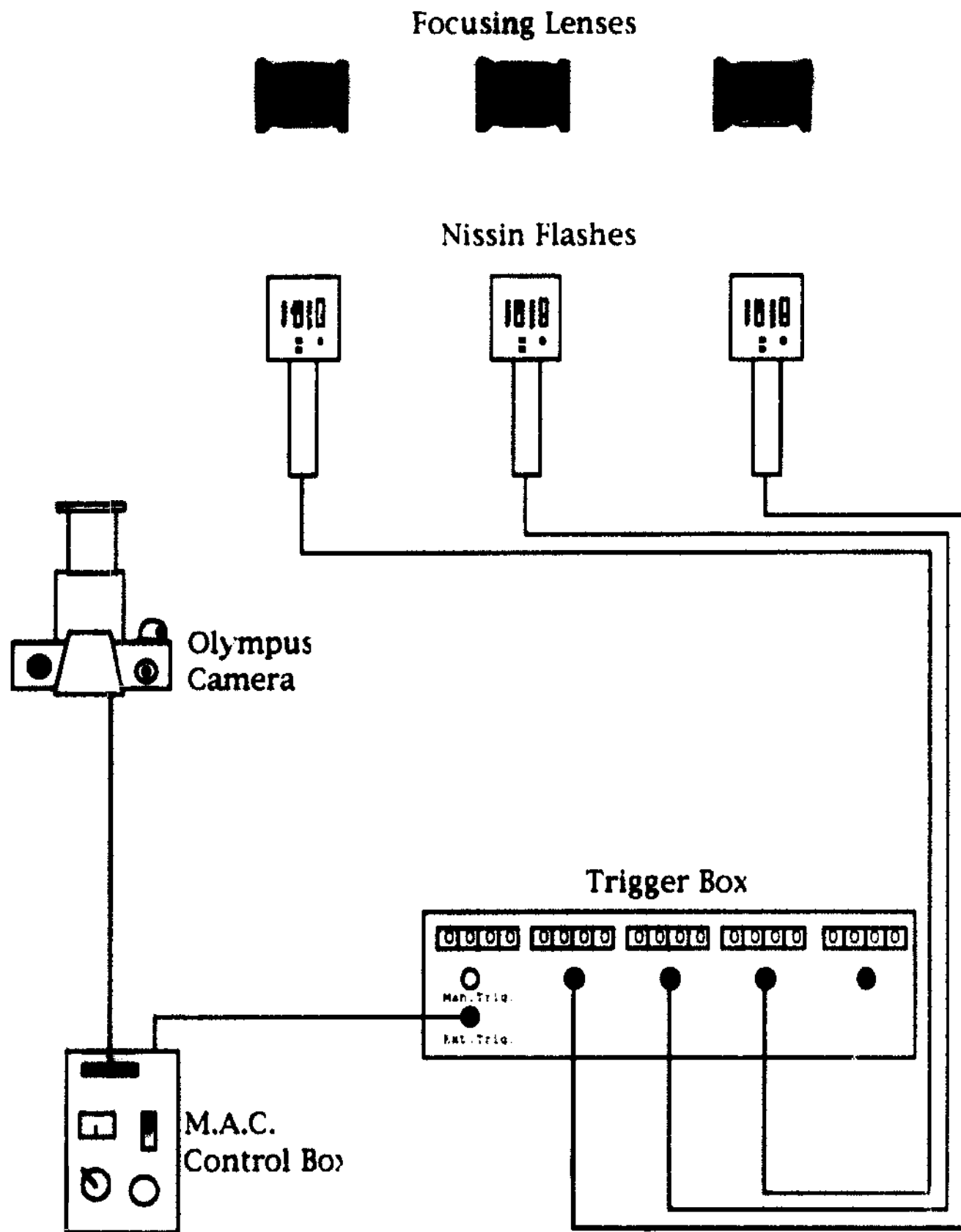
The droplets produced by the injector are illuminated by means of the flash system shown in figure 3.4. Three Nissin 4000GW flashes are staggered along a plexiglass section of the pipe down stream from the injector section. Light sheets are created by focusing the flashes through slits with spherical lenses. Except for these slits, the plexiglass flash section is covered with black plastic to prevent the illumination of other droplets outside the light sheet by scattered light. The flashes are each powered by a 9 volt power supply using aluminum cylinders as dummy batteries. The flashes are triggered sequentially with a delay between each one so as to capture three images of each droplet. The time of the delay can be calculated by the velocity of the bulk fluid and the distance between the light sheets. The delay is controlled by a triggering system that allows a range from 10 to 99990  $\mu$ s delay between each flash. The triggering system is activated by a M.A.C. control box which also sends a signal to the camera.

The camera port is located at the bottom of the test section. It contains a second collection pan which is removed as each picture is taken. Below this was an optically flat glass window through which the camera takes the photographs. The section holding the glass can be easily removed to clean off the water that accumulates on the glass.

The camera is an Olympus OM-4 with a Kiron 80-200mm macrotelephoto lens. A delay is necessary before the flashes are triggered in order to allow the shutter to open. Since the exact delay time is unknown, the shutter speed is set at 0.5 sec. and the delay is set at .075 sec. to insure that the flashes has time to trigger before the shutter closes again. The aperture and focus of the camera can be determined by trial and error. Kodak T-max 400 film is used as it is the finest grain film that can be used with the amount of light generated by the flashes.

This optical system allows photographs to be taken which show three images of each droplet. By focusing on the first image, it is possible to determine the direction of the particle. Its velocity can be determined by knowing the delay between two successive flashes and measuring the distance between the images. Figure 3.5 shows one of these photographs.

Figure 3.4: Optical System <sup>13</sup>



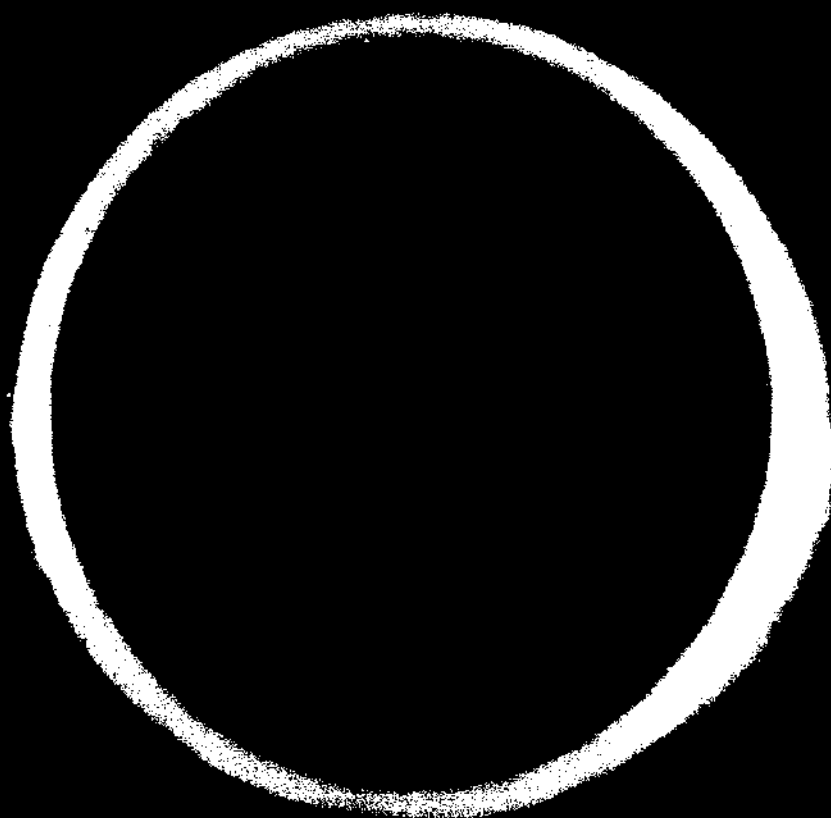


FIGURE 3.6: PHOTOGRAPH OF THE DROPLETS

Prior to running an experiment, the injector had to be inserted into the test section and aligned along the center. Lee (1987) had used a laser to do this. For this study, the alignment was judged on the uniformity of the particle deposition around the pipe wall at the flash section. The water regulator valve was opened and the frequency generator was turned on to create the droplet steam. The pins around the injector section were then used to align the injector until the deposition around the pipe circumference was even. Although not as accurate as the laser, this method gave a reasonable approximation and should not have affected the results.

After the injector was in place the compressor was started with the differential control valve shut. Air from the compressor was slowly allowed to build up pressure in the line prior to the control valve to avoid sudden pressure changes. The control valve was then slowly opened to the fraction which resulted in the desired pressure drop over the orifice.

Once both the air and water flow rates were set at desired values, the collection pan and alignment rods in the injector section were removed. Photographs were taken by quickly removing the lower droplet collection plate as the button on the M.A.C. control box was pushed, then replacing it after all three flashes triggered. In order to prevent an accumulation of water on the glass window from distorting the photographs, it was necessary to wipe it off every few frames. For the larger water flow rates associated with 150  $\mu\text{m}$  droplets with which this investigation was primarily concerned, the window had to be cleaned after each frame.

To shut down the system, the valve on the compressor was closed slowly to prevent stress in the pipe due to dramatic pressure changes. The compressor was then turned off and the pressure in the system was dissipated. The remaining valves were closed and the water to the injector was shut off. The injector was removed and stored in Nanopure purified water in the dark to prevent clogging from algae growth. Detailed step-by-step operating instructions for operation of the apparatus are outlined on page 18 of Dave Schmidt's thesis (1991).

### E. Film Developing

16

In order to use the image processing system, the negatives of the films had to be developed. Kodak T-max developer and Kodak standard fixer were used for the process. Both are sold as concentrates and had to be diluted to one gallon. Film canisters were opened in complete darkness and the films were rolled onto spools. It was possible to develop only two rolls at a time. The spools were set into a developing tank which was then covered. Once the film was in the enclosed tank, a red light could be turned on. The tank was filled with developer and agitated for five seconds out of every thirty seconds for seven minutes. Without uncovering the tank, the developer was poured out and the tank was flushed with deionized water several times. The tank was then filled with fixer and stirred constantly. After five minutes, the fixer was removed and the tank flushed with water again. The developed negatives were removed and allowed to dry.

### F. Image Processing

The image processing system used consisted of a Micro Technica TK-66 CCD shutter camera with 20 mm lens extension, a negative display stand, and a Dell System 310 computer equipped with Imagepro software. The image of a negative was sent to the computer and displayed on a video monitor. The mouse controlled a cross hair on the video monitor, the coordinates of which were displayed on the computer monitor. The coordinates of each droplet as well as three points on the pipe wall were taken manually. They were inputted along with the flash delays into a computer program which calculated concentration profiles and radial and tangential velocities. Since the coordinates were given in pixels, it was necessary to convert to squares within the program by dividing all the y-coordinates by 1.229. All calculated values were converted to fractions of pipe radius and multiplied by 2.54 cm (the pipe radius) to give concentrations in droplets per cubic centimeter and velocities in centimeters per second.

This method of determination of the particle coordinates was quicker than the previous method of using a view finder simply because it was easier to position the cross hairs with a mouse rather than to turn the knobs necessary to align the cross hairs of the view finder. The Imagepro software

This method of determination of the particle coordinates was quicker than the previous method of using a view finder simply because it was easier to position the cross hairs with a mouse rather than to turn the knobs necessary to align the cross hairs of the view finder. The Imagepro software allows for user modules to be written and used within the program. Ideally a program should have been written to analyze automatically the droplet positions and to calculate the velocities and concentrations from the image on the video monitor. Due to time constraints, the program couldn't be written.



## IV. RESULTS

The following chapter presents the results of experiments using 150 micron water droplets. The air velocity in the pipe was 1640 cm/s which resulted in a Reynolds number of 52000. The data were taken at a distance 114 cm down stream from the injector tip; the point Lee determined the particles would first begin to hit the pipe wall [3]. The concentration data are based on 998 droplets and the velocity data are based on 433 velocities.

### A. Droplet Concentrations

The concentration profile of the droplets should ideally be Gaussian. To determine the distribution, a straight line plot of the natural log of the concentration versus the squared radial fraction was made and is shown in figure 4.1. The pipe was split into ten radially equivalent sectors and the number of droplets per sector was tallied for each frame by the computer program shown in Appendix A. The number of drops per sector was totaled and divided by the volume of the sector given by the equation below to give the concentration for each sector in number per cubic centimeter.

$$V = (r_n^2 - r_{n-1}^2) \cdot \pi \cdot (\text{slit width}) \quad (4.1)$$

The radial midpoint of each sector was used as the  $r$  value for each concentration in figure 2.1. The slope of the graph gave the mean square droplet displacement from the equation

$$\text{slope} = \frac{-1}{2\overline{x_p^2}} \quad (4.2)$$

based on equation 2.17. A graph of concentration versus radial distance is shown in figure 4.2. The Gaussian distribution curve was given by

$$C = e^{-r^2/\overline{x_p^2}} \quad (4.3)$$

The mean square droplet displacement was found to be 1.12 cm<sup>2</sup>.

### B. Droplet Velocities

As can be seen from figure 3.5, in order to determine the direction of the particles, it was necessary to blur the last third image of the droplet. This

Figure 4.1: Natural Log of Concentration versus  
Radial Distance Squared

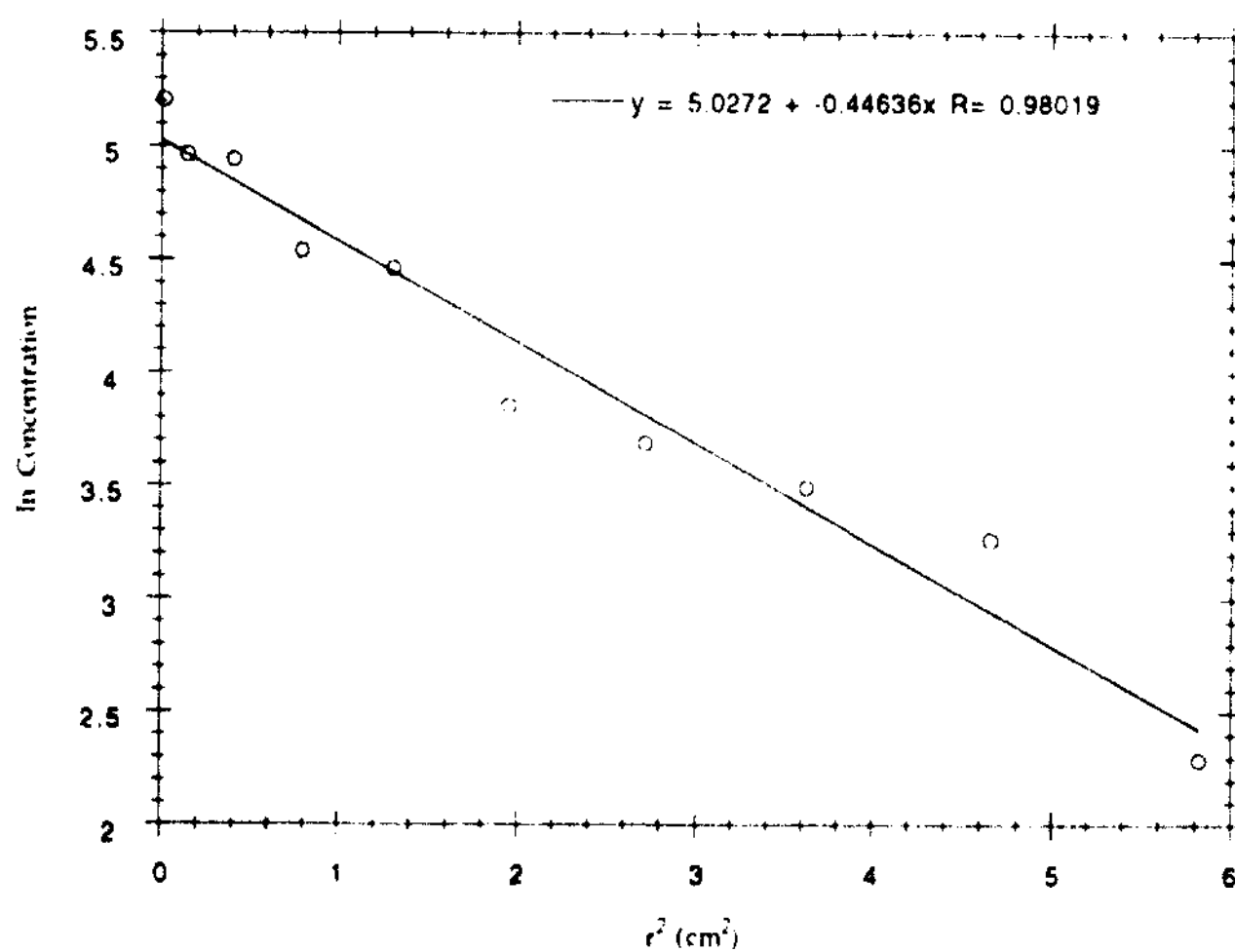
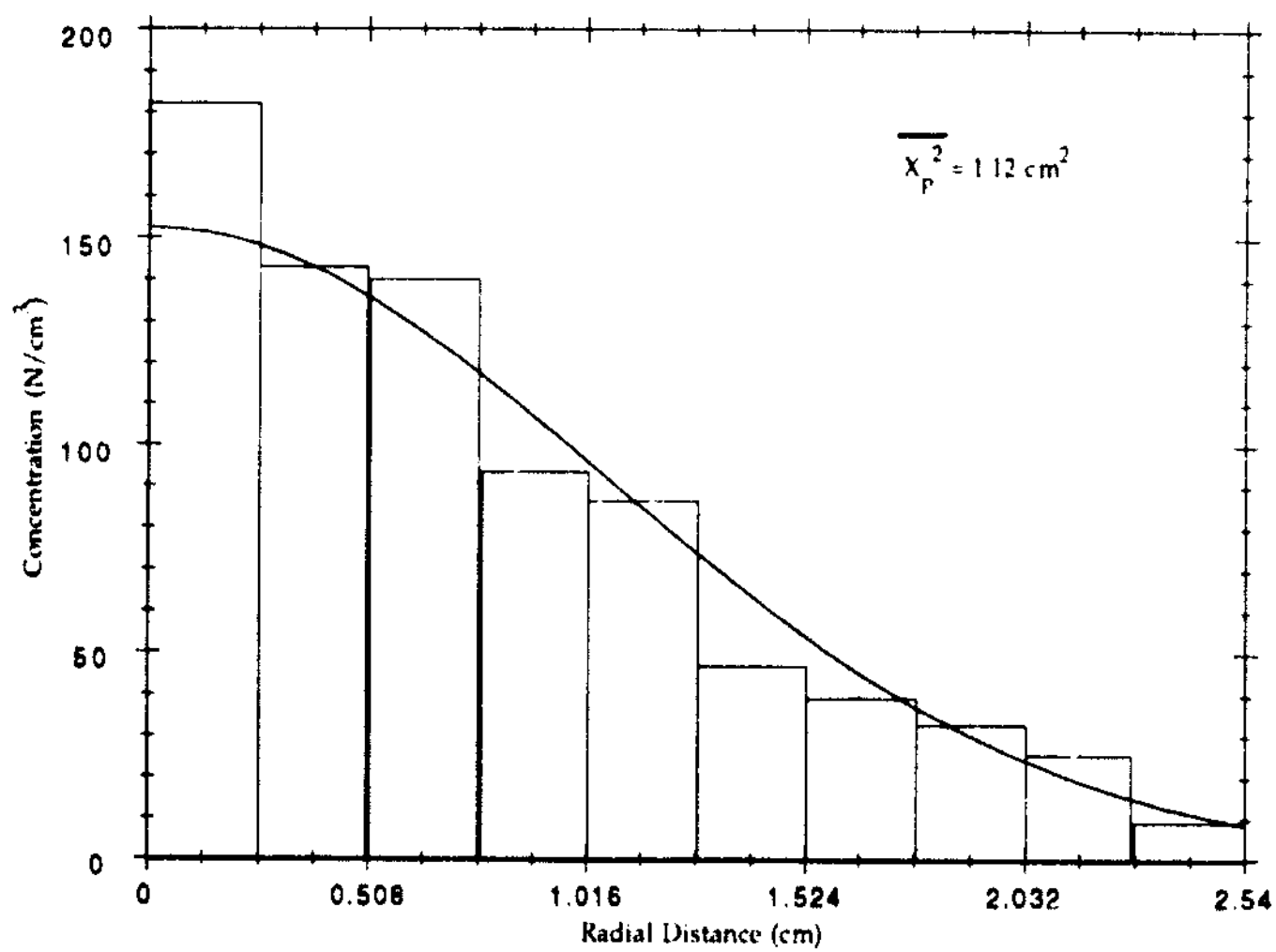


Figure 4.2: Concentration Profile



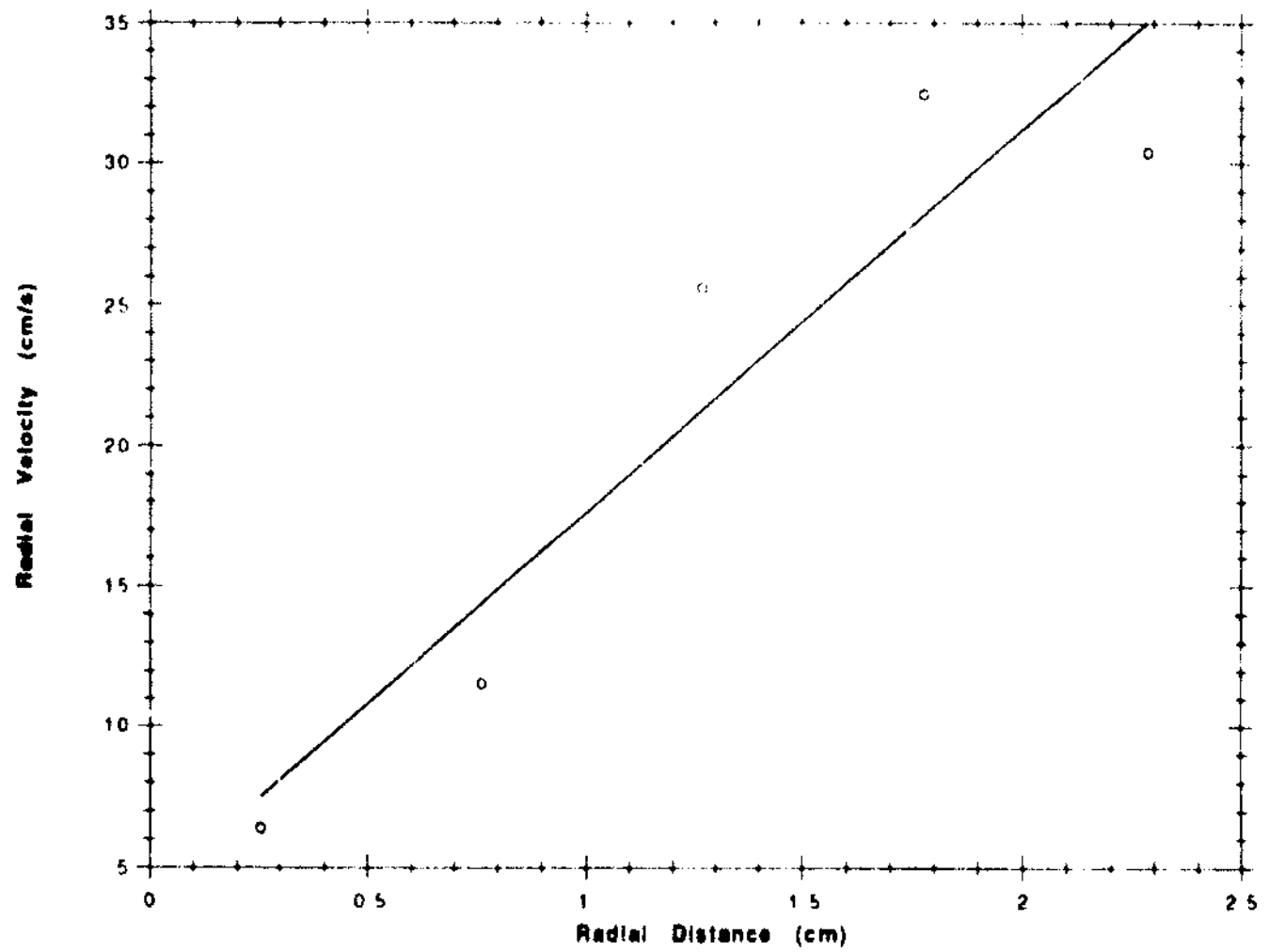
resulted in some difficulty in determining the coordinates of the center of the particles needed for velocity measurements. The blurred images didn't present a problem in the concentration calculations as the distance between sectors was large enough that an estimation of the droplet center was accurate enough. For velocity measurements the distance between droplets ranged from 1 to about 15 pixels. Therefore a much more accurate position was needed. The positions of the third images were estimated both visually and by using the computer generated darkness of each pixel with the darkest point assumed to be the center. The accuracy of the estimation is believed to be  $\pm 2$  pixels in each coordinate; therefore, the third image data were treated separately and all the calculations were carried through. It was determined that the data closely matches the data for the first and second images and it is included in the calculations shown in this report.

The results of the velocity measurements are shown in table 4.1 below. The tangential velocities should give an average of zero. Although the tangential velocities in each sector have definite values, the overall average is less than 1 cm/s. Figure 4.3 shows a plot of the radial velocity versus radial distance. The slope of the graph gives the constant  $k$  in equation 2.16 as  $13.56 \text{ s}^{-1}$ .

Tables 4.1: Measured Velocities

Radial Distance (cm)	0-.508	.508-1.016	1.016-1.524	1.524-2.032	2.032-2.540	Overall 1 Avg.
Number	47	96	117	118	55	433
$\overline{V_r}$ (cm/s)	6.4	11.54	25.56	32.49	30.38	22.65
$\overline{V_r^2}$ (cm/s) <sup>2</sup>	281.3	508.4	863.5	1340	1216	896.2
$\overline{v_r^2}$ (cm/s) <sup>2</sup>	240.3	375.2	210.2	284.4	294.3	383.2
$\overline{V_\theta}$ (cm/s)	-1.99	1.74	0.74	0.56	2.63	0.85
$\overline{V_\theta^2}$ (cm/s) <sup>2</sup>	221.1	223.6	160.6	173.3	373.7	199.9
$\overline{v_\theta^2}$ (cm/s) <sup>2</sup>	217.1	220.6	160.1	173	366.8	199.2

Figure 4.3: Radial Velocity versus Distance form the Center of the Pipe



The radial and tangential intensities were calculated by subtracting the square of the average particle velocities from the average of the squared particle velocities. The friction velocity of the fluid,  $u^*$ , was 83.93 cm/s based on a friction factor of 0.005328 and an axial velocity of 1640 cm/s calculated from equations 2.14 and 2.15. The friction velocity was used to normalize the turbulent intensities of the particles. The normalized radial and tangential intensities of the particles are plotted versus radial fraction to the wall in figures 4.4 and 4.5. The turbulent intensity of the fluid as determined by Laufer [2] is also plotted in the figures. The low values for the particle intensities in comparison to the fluid intensities show that the particles do not follow the fluid motion very well. This is primarily due to the inertia of the particles and their stopping time in the fluid. Since these particles are large compared with Lee's experiments [3] and the fluid, air, is not very viscous compared with Young's work [7] where water was used, lower normalized intensities are expected.

### C. Eddy Diffusivities

The eddy diffusivity of the particles,  $\epsilon_p$ , was found to be 15.19 cm<sup>2</sup>/s from equation 2.16 using the values calculated in the previous section. The eddy diffusivity of the fluid,  $\epsilon_f$ , was calculated from equation 2.13 using the friction velocity from above and a tube diameter of 5.08 cm. It was found to be 15.78 cm<sup>2</sup>/s. The ratio of  $\epsilon_p$  to  $\epsilon_f$  is therefore .963 and was estimated to be about one. Lee found this ratio to be 0.50 [3]. The difference in the two ratios is primarily due to the larger slope,  $k$ , found from graphing equation 2.18 which resulted in a larger particle eddy diffusivity by equation 2.16. Lee determined the value of  $k$  to be 8.33 as shown in figure 5.1.

### D. Velocity Analysis

The measured radial turbulent intensities can be compared with theoretical predictions using equation 2.6. The mean square radial fluctuation of the particles is calculated in section C above. The mean square turbulent fluctuation of the fluid, the inverse inertial time constant, and the average eddy lifetime are evaluated in the following discussion.

Figure 4.4: Radial Normalized Intensity  
as a Function of Radial Fraction

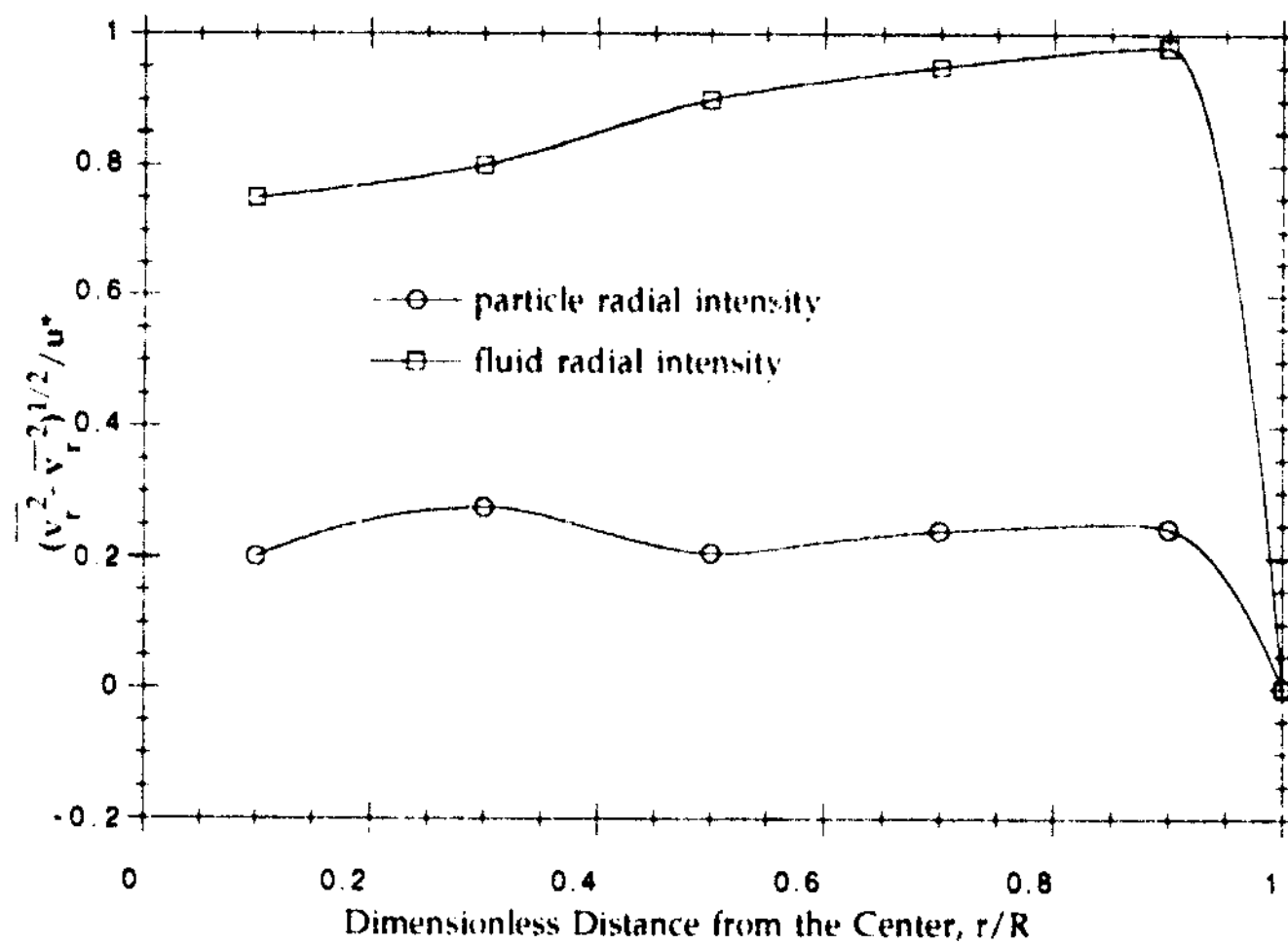
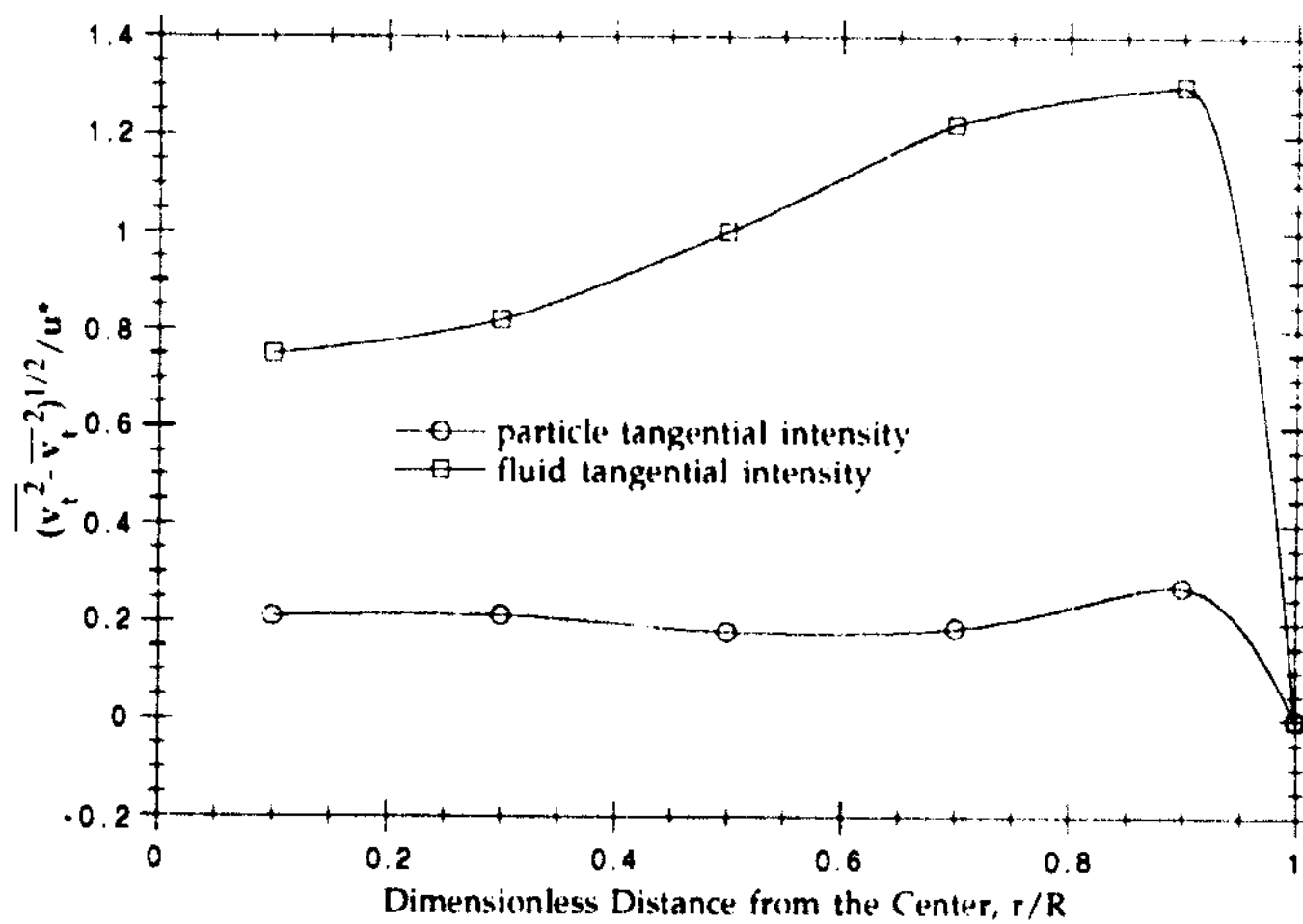


Figure 4.5: Tangential Normalized Intensity  
as a function of Radial Fraction





The mean square turbulent fluctuation of the fluid was found to be 3006 cm/s from equation 2.7. Dividing the mean square radial turbulent intensity of the particles by that of the fluid resulted in a ratio of 0.357.

The inverse inertial time constant,  $\beta$ , was evaluated using equations 2.9 through 2.11. the coefficient of drag was found to be 7.0 from table 14-6 in Bennett and Myers [1].  $\beta$  was calculated as 21.52 s<sup>-1</sup>.

The average turbulent eddy lifetime,  $\tau_t$ , was calculated from equation 2.12 to be 0.00481 sec using the fluid eddy diffusivity and fluid mean square fluctuation calculated above. Evaluating equation 2.6 with the calculated values of  $\beta$  and  $\tau_t$  gives a predicted value of 0.344. Even though equation 2.6 is a square root function, it gives acceptable agreement between the predicted and experimentally determined ratios of particle to fluid turbulent intensities.

## V. DISCUSSION

### A. Velocity Measurements

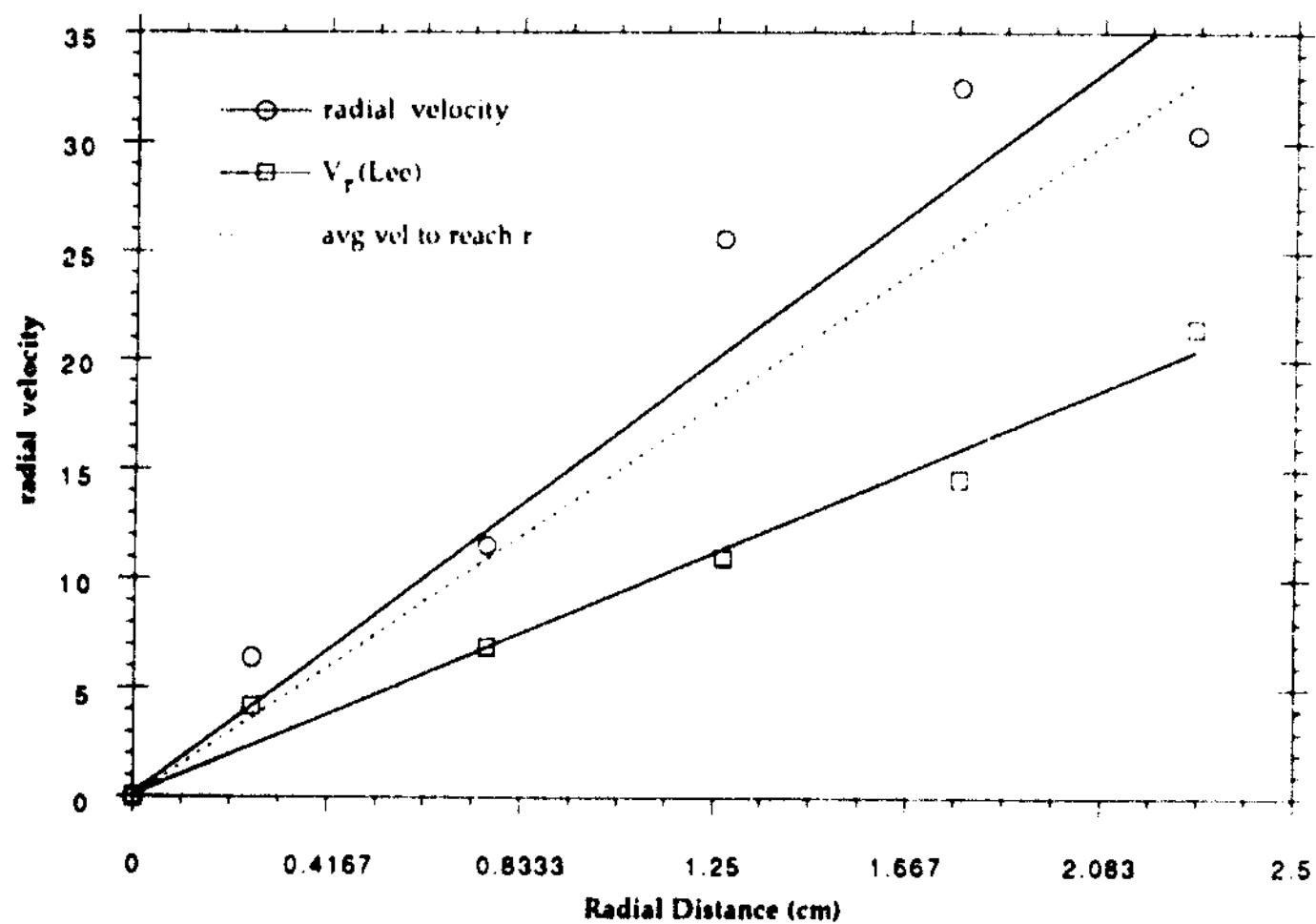
The differences between the measurements of  $\epsilon_p$  in this investigation and the results of Michael Lee [3] are a direct result of the different values acquired for the radial velocities in the two studies. The radial velocity results are compared with Lee's experiments in figure 5.1. Also graphed is the average radial velocity required for a particle to travel from the center of the pipe to each radial distance calculated from

$$v_r = U_f \cdot r / z \quad (5.1)$$

where  $z$  is the axial distance downstream of the injector; 114 cm in this case. The calculated average velocities give a good estimate of the minimum average velocity of the particles, although the actual velocities should be closer to the estimated values when the particles are above the average overall radial velocity. The graph shows that the velocities found in this study are reasonable. It follows therefore that the particle eddy diffusivity calculated using these data is also reasonable.

The correlation developed by Lee (equation 2.6) [3] is a comparison of the theoretical and experimental values for the ratio of the turbulent intensity of the particles to the turbulent intensity of the fluid. Although the radial velocities measured in Lee's study were considerably lower, the turbulent radial intensities calculated for the particles in both experiments were closer. Lee calculated the root mean square radial particle fluctuation to be 21.91 cm/s where it was found to be 19.57 cm/s in this thesis. These values resulted in root particle to fluid intensity ratios of 0.36 and 0.357 respectively. Compared with the theoretically predicted value of 0.344, both of these values are reasonable. It is interesting to note that difference in radial velocities between the two sets of measurements had little overall effect except to the particle diffusion coefficient.

Figure 5.1: Comparison of Radial Velocities



### B. Particle Deposition

Lee's particle deposition model was discussed in section A of chapter one. It was shown that by knowing the eddy diffusion and the radial intensity of the particles, it was possible to predict the fraction deposition as a function of time.

Lee developed a computer program to evaluate the particle deposition model by solving equation 2.4. It is listed in Appendix A. The constants needed for the program are the particle eddy diffusivity and the mean square radial intensity within one stopping distance from the wall. The eddy diffusivity is shown in chapter five to be  $15.19 \text{ cm}^2/\text{s}$ . To calculate mean square radial intensity, the stopping distance had to be found. The stopping distance,  $\delta$ , of a particle is dependent on its inertia and is therefore calculated from the inverse inertial time constant by the equation

$$\delta = \left(\frac{1}{\beta}\right)(\overline{v_r^2})^{1/2} \quad (5.2)$$

The stopping distance was found to be 1.009 cm which is equivalent to a radial fraction of 0.603 from the center of the pipe. It was possible to determine the normalized radial intensity of the particles one stopping distance from the wall from the graph of particle radial mean square velocity versus radial fraction shown in figure 5.3. Inputting the constants into the computer program resulted in the graph of the fraction of droplets deposited on the wall as a function of time shown in figure 5.4.

Figure 5.3: Root Mean Square Radial Velocity versus Radial Fraction

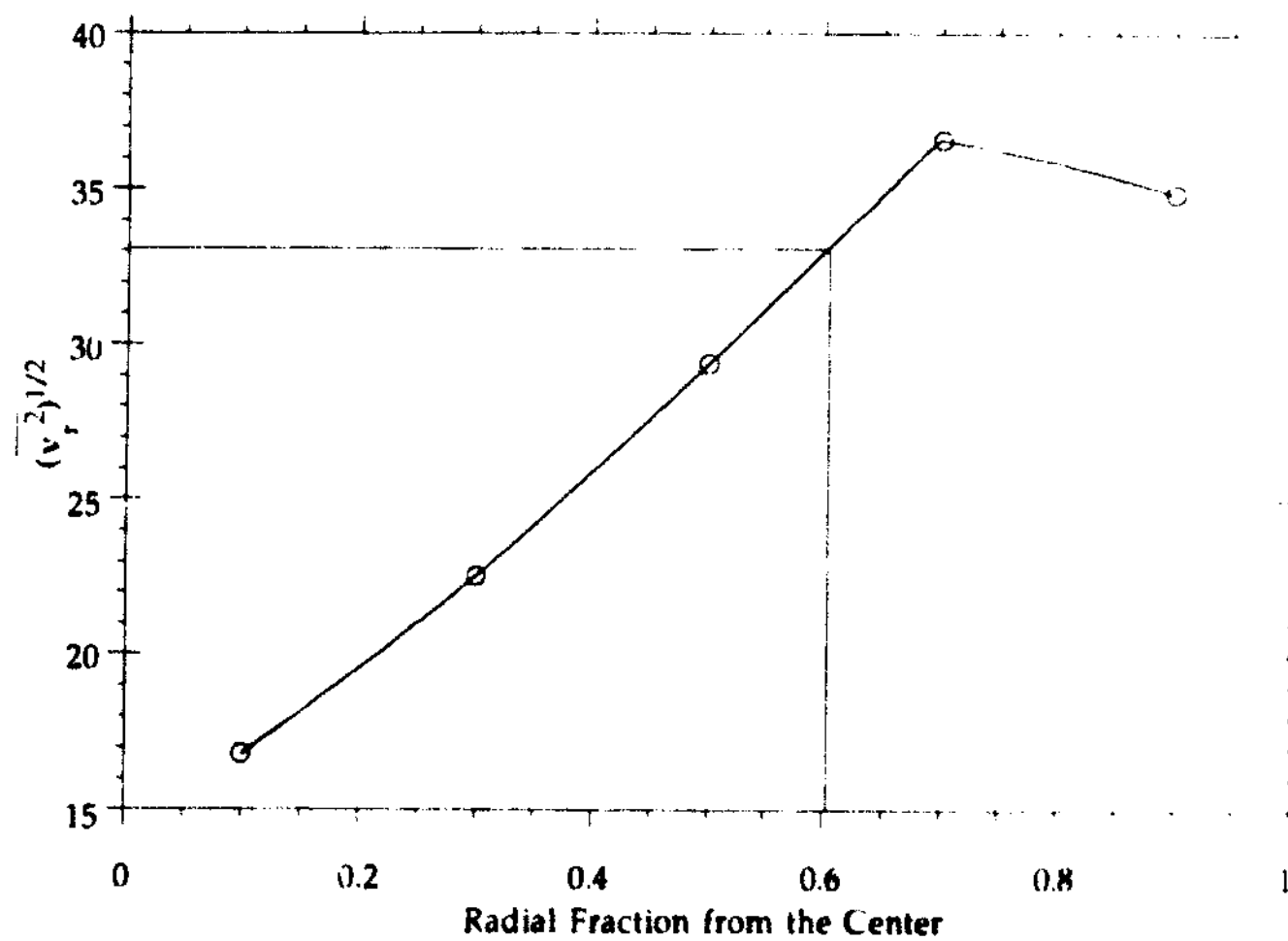
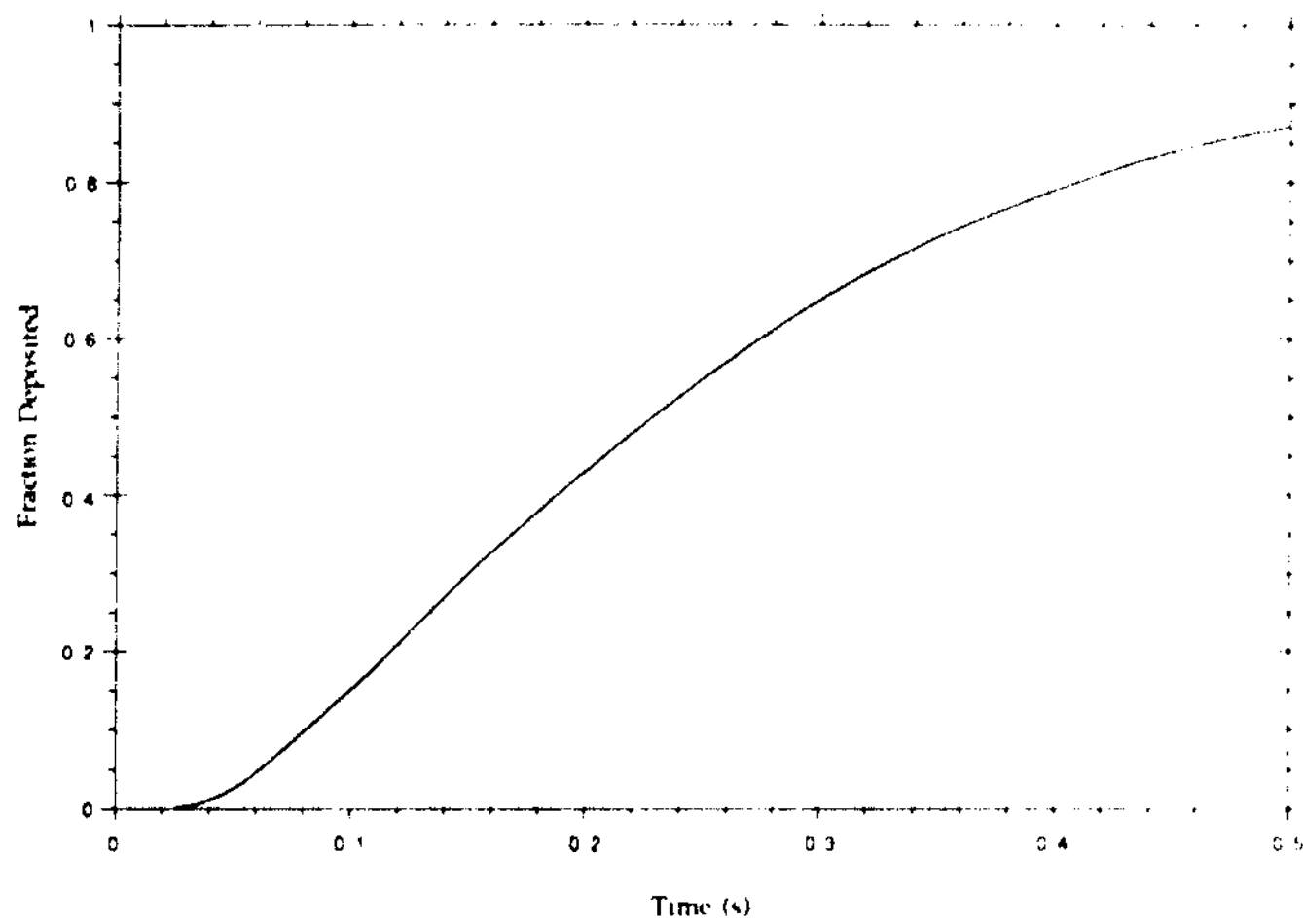


Figure 5.4: Fraction of Droplets Deposited versus Time



**Appendix A:**  
**Program Listings**

```

      PROGRAM HANRATTY
C *****
C *
C * THIS PROGRAM GIVES THE NUMBER OF IMAGES IN EACH RADIAL SECTOR
C * AND CALCULATES RADIAL AND TANGENTIAL VELOCITY COMPONENTS
C *
C *****

C ----- PIPE CENTER VARIABLES -----NNN-----
      REAL XP1,YP1,XP2,YP2,XP3,YP3,XPA,YPA,XPB,YPB,XP,YP,
C ----- IMAGE COORDINATE VARIABLES -----
      * X1(30),Y1(30),X2(30),Y2(30),X3(30),Y3(30),
C ----- RADIUS VARIABLES -----
      * RAD,R1(30),R2(30),R3(30),RR1,RR2,RR3
C ----- OTHER VARIABLES -----
      REAL DIV,RVEL1(30),TVEL1(30),RVEL2(30),TVEL2(30),TIME1,TIME2,
      * T1,T2,T3,T4,TIM1,TIM2
      CHARACTER*4 NAME
      INTEGER X,Y,Z,RAD1,RAD2,RAD3,C(30),X11,X12,X13,Y11,Y12,Y13,TIMO

C ----- DIV= PIXELS/IN (Y) / PIXELS/IN (X) -----
      DIV=1.229
      7 DO 231 X=1,30
        C(X)=0
        X1(X)=0
        X2(X)=0
        X3(X)=0
        Y1(X)=0
        Y2(X)=0
        Y3(X)=0
        RVEL1(X)=0
        RVEL2(X)=0
        TVEL1(X)=0
        TVEL2(X)=0
      231 CONTINUE

      WRITE(*,*) 'ENTER FRAME NUMBER IN SINGLE QUOTES'
      READ(*,*) NAME

C ----- TIME BETWEEN IMAGES -----
      TIM1=TIME1
      TIM2=TIME2
      WRITE(*,*) 'ENTER TIME BETWEEN FIRST AND SECOND IMAGES (SEC)'
      READ(*,*) TIME1
      IF (TIME1.LE.0) TIME1=TIM1
      WRITE(*,*) 'ENTER TIME BETWEEN SECOND AND THIRD IMAGES (SEC)'
      READ(*,*) TIME2
      IF (TIME2.LE.0) TIME2=TIM2

C ----- PIPE WALL COORDINATES -----
      23 WRITE(*,*) 'ENTER WALL COORDINATES: (X1,Y1,X2,Y2,X3,Y3)'
      READ(*,*) XP1,YP1,XP2,YP2,XP3,YP3
      WRITE(*,*) '0 TO GO ON'
      READ(*,*) Y
      IF (Y.NE.0) GOTO 23
      YP1=YP1/DIV

```



YP2=YP2/DIV  
YP3=YP3/DIV

```
C ----- IMAGE POSITIONS -----  
  WRITE(*,*) 'ENTER DROPLET POSITIONS:'  
  WRITE(*,*) ' 1, 2, AND 3 INDICATE IMAGES OF THE SAME DROP'  
  WRITE(*,*) ' ENTER 0 TO MOVE TO NEXT DROPLET'  
  WRITE(*,*) ' ENTER 0 ON IMAGE 1 TO QUIT DATA ENTRY'  
  WRITE(*,*) 'USE ONLY 1-13 FOR VELOCITIES'  
  DO 50 X=1,30  
40  WRITE(*,*) 'ENTER X1(',X,'):'  
    READ(*,*) X1(X)  
    IF(X1(X).EQ.0) GOTO 1  
    Z=X  
    WRITE(*,*) 'ENTER Y1(',X,'):'  
    READ(*,*) Y1(X)  
    WRITE(*,*) 'ENTER X2(',X,'):'  
    READ(*,*) X2(X)  
    IF (X2(X).EQ.0) GOTO 50  
    WRITE(*,*) 'ENTER Y2(',X,'):'  
    READ(*,*) Y2(X)  
    WRITE(*,*) 'ENTER X3(',X,'):'  
    READ(*,*) X3(X)  
    IF (X3(X).EQ.0) GOTO 50  
    WRITE(*,*) 'ENTER Y3(',X,'):'  
    READ(*,*) Y3(X)  
50  CONTINUE  
    1 DO 91 TIMO=1,25  
      WRITE(*,*) ' '  
91  CONTINUE  
    WRITE(*,*) '          THESE ARE THE ENTERED COORDINATES:'  
    DO 51 Y=1,2  
      XI1=INT(X1(Y))  
      XI2=INT(X2(Y))  
      XI3=INT(X3(Y))  
      YI1=INT(Y1(Y))  
      YI2=INT(Y2(Y))  
      YI3=INT(Y3(Y))  
      WRITE(*,17) Y,XI1,YI1,XI2,YI2,XI3,YI3  
17  FORMAT(10X,' DROP ',I2,':  (' ,I4,',',I4,') (' ,I4,',',  
    * I4,') (' ,I4,',',I4,')')  
51  CONTINUE  
    2  WRITE(*,*) '          ENTER A DROP # TO CHANGE OR 0 TO GO ON'  
      READ(*,*) Y  
      IF(Y.GT.2) THEN  
        GOTO 2  
      ELSEIF(Y.NE.0) THEN  
        WRITE(*,*) 'ENTER X1(',Y,'):'  
        READ(*,*) X1(Y)  
        WRITE(*,*) 'ENTER Y1(',Y,'):'  
        READ(*,*) Y1(Y)  
        WRITE(*,*) 'ENTER X2(',Y,'):'  
        READ(*,*) X2(Y)  
        WRITE(*,*) 'ENTER Y2(',Y,'):'  
        READ(*,*) Y2(Y)  
        WRITE(*,*) 'ENTER X3(',Y,'):'
```

```

      READ(*,*) X3(Y)
      WRITE(*,*) 'ENTER Y3(' ,Y, '): '
      READ(*,*) Y3(Y)
      GOTO 1
    ENDIF
    TIMO=2
    DO 52 Y=1,Z
      Y1(Y)=Y1(Y)/DIV
      Y2(Y)=Y2(Y)/DIV
      Y3(Y)=Y3(Y)/DIV
52  CONTINUE
    DO 99 Y=(Z+1),30
      X1(Y)=0
      X2(Y)=0
      X3(Y)=0
      Y1(Y)=0
      Y2(Y)=0
      Y3(Y)=0
99  CONTINUE

C ----- CALCULATE PIPE CENTER AND RADIUS -----
C -----
C - CENTER IS FOUND FORM THE INTERSECTION OF THE PERPENDICULAR
C   BISECTORS OF THE CHORDS DEFINED BY THE THREE POINTS ENTERED

      XPA=DABS((XP3+XP2)/2)
      YPA=DABS((YP3+YP2)/2)
      XPB=DABS((XP2+XP1)/2)
      YPB=DABS((YP2+YP1)/2)
      XP=(YPA-YPB-((XP2-XP3)/(YP3-YP2))*XPA+((XP1-XP2)/(YP2-YP1))*
      * XPB)/(((XP1-XP2)/(YP2-YP1))-((XP2-XP3)/(YP3-YP2)))
      YP=((XP2-XP3)/(YP3-YP2))*XP+YPA-((XP2-XP3)/(YP3-YP2))*XPA

      RAD=((XP-XP1)**2+(YP-YP1)**2)**0.5

C ----- CONCENTRATION PROFILE -----
C -----
C - SET R2 AND R3 EQUAL TO ZERO WHEN NO DATA IS GIVEN

      DO 53 X=1,Z
      R1(X)=((XP-X1(X))**2+(YP-Y1(X))**2)**0.5/RAD
      IF (X2(X).EQ.0) THEN
        R2(X)=0
      ELSE
        R2(X)=((XP-X2(X))**2+(YP-Y2(X))**2)**0.5/RAD
      ENDIF
      IF (X3(X).EQ.0) THEN
        R3(X)=0
      ELSE
        R3(X)=((XP-X3(X))**2+(YP-Y3(X))**2)**0.5/RAD
      ENDIF

C ----- LOOP TO FIND CONCENTRATIONS AT VARYING RADII -----
C - A RADIUS OF ZERO WILL NOT BE ADDED INTO THE CCNCENTRATIONS
      DO 63 Y=1,10
      RR1=R1(X)*10

```

```

RR2=R2(X)*10
RR3=R3(X)*10
IF ((RR1.GT.(Y-1)).AND.(RR1.LE.Y)) THEN
  C(Y)=C(Y)+1
ENDIF
IF ((RR2.GT.(Y-1)).AND.(RR2.LE.Y)) THEN
  C(Y)=C(Y)+1
ENDIF
IF ((RR3.GT.(Y-1)).AND.(RR3.LE.Y)) THEN
  C(Y)=C(Y)+1
ENDIF
63 CONTINUE
53 CONTINUE

C ----- VELOCITIES -----
C -----
? - PROJECT THE VELOCITY VECTOR ON TO A RADIAL VECTOR DRAWN FROM
C THE CENTER OF THE PIPE TO THE MIDPOINT OF THE VELOCITY VECTOR

DO 54 X=1,2
  IF (X2(X).EQ.0) GOTO 54
  XC=(X1(X)+X2(X))/2
  YC=(Y1(X)+Y2(X))/2

C - COMP (b) A A (DOT) B / (MAGNITUDE) B
  T1=((X2(X)-X1(X))*(XC-XP))+((Y2(X)-Y1(X))*(YC-YP))/
  * (((XC-XP)**2+(YC-YP)**2)**0.5)
  RVEL1(X)=(T1*2.54)/(RAD*TIME1)
  T2=((X2(X)-X1(X))*(YP-YP))+((Y2(X)-Y1(X))*(XC-XP))/
  * (((XC-XP)**2+(YC-YP)**2)**0.5)
  TVEL1(X)=(T2*2.54)/(RAD*TIME1)
54 CONTINUE
DO 64 X=1,2
  IF (X3(X).EQ.0) GOTO 64
  XC=(X2(X)+X3(X))/2
  YC=(Y2(X)+Y3(X))/2
  T3=((X3(X)-X2(X))*(XC-XP))+((Y3(X)-Y2(X))*(YC-YP))/
  * (((XC-XP)**2+(YC-YP)**2)**0.5)
  RVEL2(X)=(T3*2.54)/(RAD*TIME1)
  T4=((X3(X)-X2(X))*(YP-YP))+((Y3(X)-Y2(X))*(XC-XP))/
  * (((XC-XP)**2+(YC-YP)**2)**0.5)
  TVEL2(X)=(T4*2.54)/(RAD*TIME1)
64 CONTINUE

C ----- GIVE RESULTS -----
C -----
DO 92 TIMO=1,25
  WRITE(*,*) ' '
92 CONTINUE
  WRITE(*,*) ' FRAME- ',NAME,' RADIUS (X-PIXELS) = ',RAD
  WRITE(*,101)C(1),C(2)
101 FORMAT(15X,'C1 (.254cm) =',I2,' C2 (.254-.508cm) =',I2)
  WRITE(*,1(2)C(3),C(4)
102 FORMAT(15X,'C3 (.508-.762cm) =',I2,' C4 (.762-1.016cm) =',I2)
  WRITE(*,103)C(5),C(6)
103 FORMAT(15X,'C5 (1.016-1.270cm) =',I2,' C6 (1.270-1.524cm) =',I2)

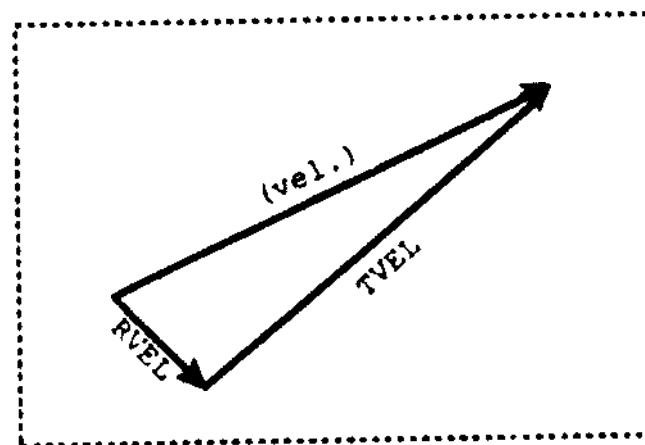
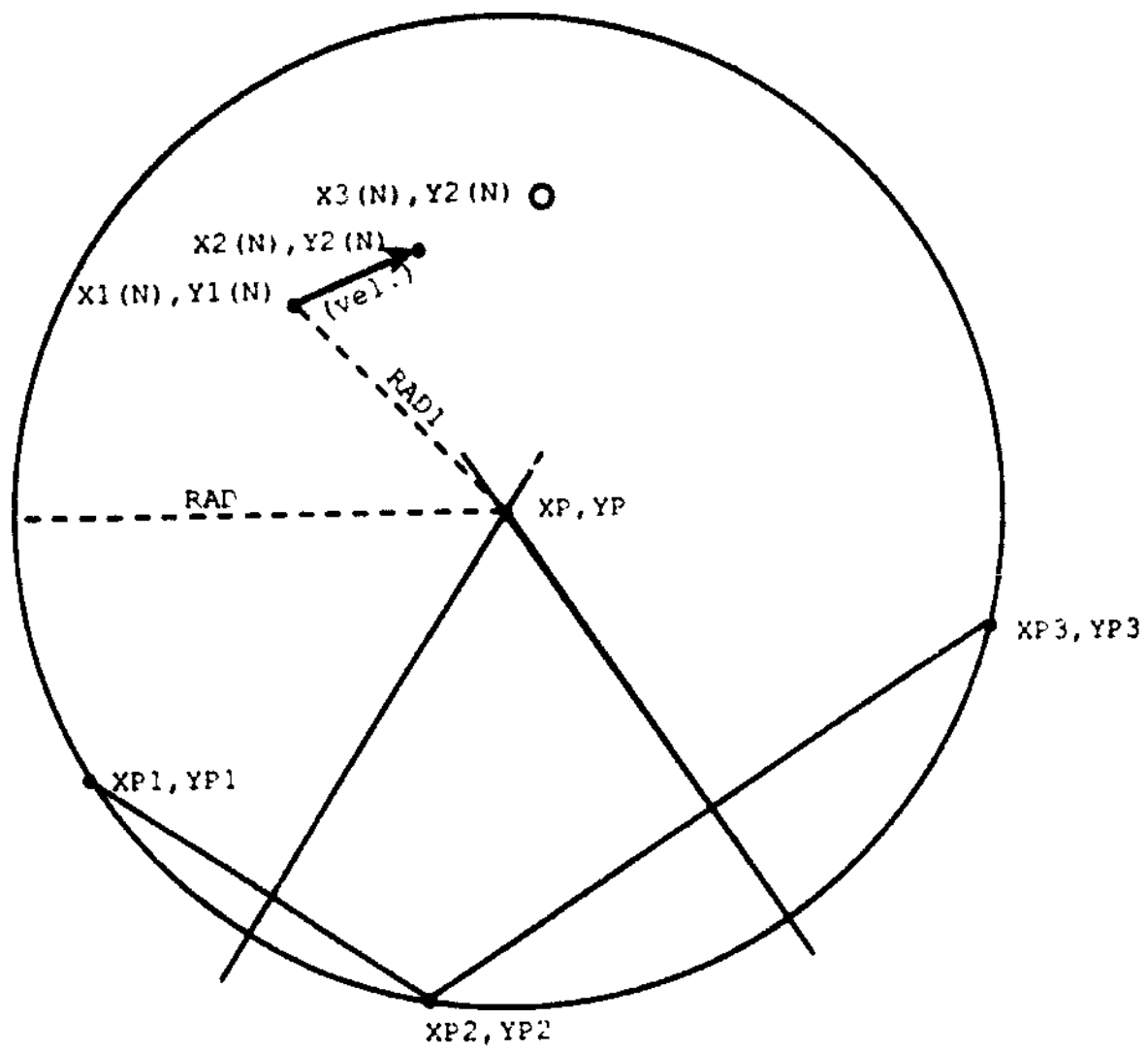
```

```

WRITE(*,104)C(7),C(8)
104 FORMAT(15X,'C7(1.524-1.778cm)=' ,I2,' C8(1.778-2.032cm)=' ,I2)
WRITE(*,105)C(9),C(10)
105 FORMAT(15X,'C9(2.032-2.286cm)=' ,I2,' C10(2.286-2.54cm)=' ,I2)
WRITE(*,*)
WRITE(*,*) '          POINT 1    POINT 2    POINT 3    RAD1-2',
*' TAN1-2  RAD2-3  TAN2-3'
DO 71 X=1,14
IF (X1(X).EQ.0) THEN
GOTO 71
ELSE
RAD1=INT((((X1(X)-XP)**2+(Y1(X)-YP)**2)**0.5)*100/RAD)
ENDIF
IF (X2(X).EQ.0) THEN
RAD2=INT(0)
ELSE
RAD2=INT((((X2(X)-XP)**2+(Y2(X)-YP)**2)**0.5)*100/RAD)
ENDIF
IF (X3(X).EQ.0) THEN
RAD3=INT(0)
ELSE
RAD3=INT((((X3(X)-XP)**2+(Y3(X)-YP)**2)**0.5)*100/RAD)
ENDIF
WRITE(*,106) RAD1,RAD2,RAD3,RVEL1(X),TVEL1(X),RVEL2(X),TVEL2(X)
106 FORMAT(10X, 18, 2X, 18, 2X, 18, 2X, F6.2, 2X,
* F6.2, 2X, F6.2, 2X, F6.2)
71 CONTINUE
31 WRITE(*,*) '          1-VIEW COORDINATES, 2-START OVER, 3-DONE'
READ(*,*) X
IF (X.EQ.1) THEN
DO 312 X=1,30
Y1(X)=Y1(X)*DIV
Y2(X)=Y2(X)*DIV
Y3(X)=Y3(X)*DIV
312 CONTINUE
GOTO 1
ENDIF
IF (X.EQ.2) GOTO 7
IF (X.NE.3) GOTO 31
STOP
END

```

Figure A.1: Program Variables



```

C*****
C*****
C
C THIS PROGRAM CALCULATES THE MEAN AXIAL VELOCITY, MASS FLOW RATE AND
C REYNOLDS NUMBER IN A PIPE
C
C COURTESY OF DR. J. S. VAMES
C*****
C
C INPUT PARAMETERS  1) ORIFICE DIAMETER IN THE ORIFICE PLATE, D2
C                   2) DIAMETER OF THE LINE FOR WHICH THE ORIFICE PLATE
C                     IS LOCATED, L
C                   3) DIAMETER OF THE TEST SECTION, DT
C                   4) STATIC PRESSURE IN THE TEST SECTION, H0
C                   5) TEMPERATURE IN THE TEST SECTION, T0
C                   6) ATMOSPHERIC PRESSURE, PA
C                   7) LINE PRESSURE AND TEMPERATURE BEFORE THE ORIFICE
C                     PLATE, P1 AND T1
C                   8) PRESSURE DROP OVER THE ORIFICE PLATE, DELH2
C                   9) ORIFICE COEFFICIENT, COF
C*****
C
C OUTPUT           1) MASS FLOW RATE
C                   2) MEAN AXIAL VELOCITY
C                   3) FLUID REYNOLDS NUMBER BASED ON PIPE DIAMETER AND
C                     MEAN AXIAL VELOCITY
C*****
C INPUT DIXED DATA, PIPE AND ORIFICE SIZE
C REAL L
C PRINT*, 'ORIDICE DIAM.(IN), LINE SIZE(IN), TEST SECTION DIAM.(IN),
C READ*, D2, L, DT
C B=D2/L
15 PRINT*, 'STATIC PRESSURE IN TEST SECTION (CM), SPG?'
C READ*, H0, SPG0
C PRINT*, 'TEMPERATURE, T0 (DEG C)'
C READ*, T0
C PRINT*, 'ATMOSPHERIC PRESSURE (MM HG)'
C READ*, PA
C P0=62.4*(H0/2.54)*SPG0/12+(PA/760*2116.224)
C INPUT ORIFICE DATA
C PRINT*, 'UPSTREAM PRESS (PSIG), TEMP (DEG C)'
C READ*, P1, T1
70 PRINT*, 'PRESSURE DROP OVER ORIFICE (CM), SPG?'
C READ*, DEL H2, SPG2
C CALCULATE ORIFICE COEFFICIENT
C A0=3.141592654*(DT**2)/576
C A2=3.141592654*(D2**2)/576
C DELP2=62.4*(DELH2/2.54)*SPG2/12
C PA=PA/760*14.696

```

```

DEN1=.001205*62.43*(293.13/(T1+273.13))*((P1+PA)/14.696)
R=(P1-(DELP2/144))/P1
Y=1-((1-R)/1.4)*(.41+.35*(B**4))
F=SQRT((1-(B**4))/(2*32.17*DELP2*DEN1))
50 PRINT*, 'GIVE ORIFICE COEFFICIENT'
   READ*, COF
   W=COF*Y*A2/F
   VAVE=W/(DEN0*A0)
   RE=(DT/12)*VAVE*DEN0/1.2499E-5
   PRINT*, 'W=', W, 'LBM/S', 'VAVE=', VAVE, 'FT/S', 'RE=', RE
   PRINT*, ' '
   PRINT*, 'CONTINUE? 1(YES) 0(NO)'
   READ*, FLAG
   IF (FLAG.EQ.0) GOTO 60
   GOTO 50
60 STOP
   END

```

```

C*****
C*
C*  THIS PROGRAM CLACULATES THE FRACTION OF THE DROPLETS DEPOSITED
C*  ON THE WALL BY SOLVING THE DIFFUSION EQUATION
C*
C*  COURTESY DR. MICHAEL LEE
C*****
C*  BOUNDRY CONDITION AT THE WALL:
C*    -Dp(dC/dr)=(1/SQRT(2*3.1416))*(SQRT(Vr**2))*C
C*****
C*  INPUT PARAMETERS: 1.) PIPE RADIUS, RAD
C*                    2.) DROPLET DIFFUSION COEFFICIENT, D
C*                    3.) TURBULENT INTENSITY OF THE DROPLETS WITHIN
C*                      ONE STOPPING DISTANCE OF THE WALL, VP
C*                    4.) NUMBER OF FOURIER CONSTANTS DESIRED, NROOTS
C*                    5.) INITIAL GUESS TO SOLVE THE NEWTON-RAPHSON
C*                      METHOD (0.3 IS A REASONABLE VALUE), ALFA0
C*                    6.) THE INTERVAL BETWEEN THE FOURIER COEFFICIENTS
C*                      (1.16 IS A REASONABLE VALUE), ALIN
C*****
      PROGRAM LEE
      DIMENSION ALFA(30)
      REAL MMBSJ1,MMBSJ0,ARG,X1
      WRITE(*,*)'ENTER THE PIPE RADIUS (CM)'
      READ(*,*) RAD
      WRITE(*,*)'ENTER THE DIFFUSION COEFFICIENT'
      READ(*,*) D
      WRITE(*,*)'ENTER THE TURBULENT INTENSITY OF THE DROPLETS'
      READ(*,*) VP
      WRITE(*,*)'ENTER THE NUMBER OF ROOTS OF THE BESSEL FUNCTION'
      READ(*,*) NROOTS
      WRITE(*,*)'ENTER NUMBER OF TIME INCREMENTS'
      READ(*,*) NSTEP
      WRITE(*,*)'ENTER THE STARTING TIME'
      READ(*,*) T0
      WRITE(*,*)'ENTER FINAL TIME'
      READ(*,*) TF
      WRITE(*,*)'ENTER ALFA0'
      READ(*,*) ALFA0
      WRITE(*,*)'ENTER ALFA0 INCREMENT'
      READ(*,*) ALIN
      VP=VP/(SQRT(2*3.1456))
      DT=(TF-T0)/NSTEP
C*****
C***  SOLVE FOR THE FOURIER CONSTANTS USING NEWTON-RAPHSON'S
C***  TECHNIQUE ONLY IN THE FIRST TIME STEP.  THE RESULTS ARE
C***  STORED IN AN ARRAY, ALFA(N).
C*****
      DO 20 K=1,NSTEP
      SUM=0.0
      T=DT*(K-1)+T0
      DO 30 J=1,NROOTS
      IF(K.NE.1) GOTO 40
      IF(J.NE.1) GOTO 50
      ALFA0=ALFA(J-1) + ALIN
50    CALL NEWTON(ALFA0,A,D,VP,RAD)

```



```

      ALFA(J)=-A
C*****
C***  SOLVE FOR EQUATION (3.15) IN CHAPTER 3 (LEE'S THESIS)      *
C*****
40   ARG0=RAD*ALFA(J)
      ARG1=RAD*ALFA(J)
      X0=MMBSJ0(ARG0,IER)
      X1=MMBSJ1(ARG1,IER)
      COEF=-D*T*(ALFA(J)**2)
      COEF1=-D*T0*(ALFA(J)**2)
      DENO = ALFA(J)*(X0**2+X1**2)
      SUM=SUM+X1*(EXP(COEF1)-EXP(COEF))/DENO
30   CONTINUE
      FRAC=2*SUM/RAD
      WRITE(*,*)T,FRAC
20   CONTINUE
C*****
C***  CHECK IF THE FOURIER CONSTANTS ARE CORRECT BY      *
C***  SUBSTITUTING THE VALURES INTO THE EXPRESSION FOR F(ALFA)  *
C*****
      DO 60 II=1,NROOTS
      AARG0=RAD*ALFA(II)
      AARG1=RAD*ALFA(II)
      X0=MMBSJ0(AARG0,IER)
      X1=MMBSJ1(AARG1,IER)
      BC=D*ALFA(II)*X1-X0*VP
      WRITE(*,*) ALFA(II),BC
60   CONTINUE
      STOP
      END
C*****
C***  THIS SUBROUTINE SOLVES FOR THE FOURIER CONSTANTS USING THE  *
C***  NEWTON-RAPHSON'S TECHNIQUE      *
C*****
      SUBROUTINE NEWTON(ALFA0,A,D,VP,RAD)
      REAL MMBSJ0,MMBSJ1
      ALFA1=ALFA0
10   ARG0=RAD*ALFA1
      X0=MMBSJ0(ARG0,IER)
      ARG1=RAD*ALFA1
      X1=MMBSJ1(ARG1,IER)
      F=D*ALFA1*X1-X0*VP
      FPRIME=D*RAD*ALFA1*X0+RAD*VP*X1
      ALFA2=ALFA1-F/FPRIME
      DEL=ALFA2-ALFA1

      IF(ABS(DEL).LE.0.001) GOTO 100
      ALFA1=ALFA2
      GOTO 10
100  A=ALFA2
      RETURN
      END

```

**Appendix B:**  
**Calibration Charts**

**Figure B1: Rotameter Calibration**

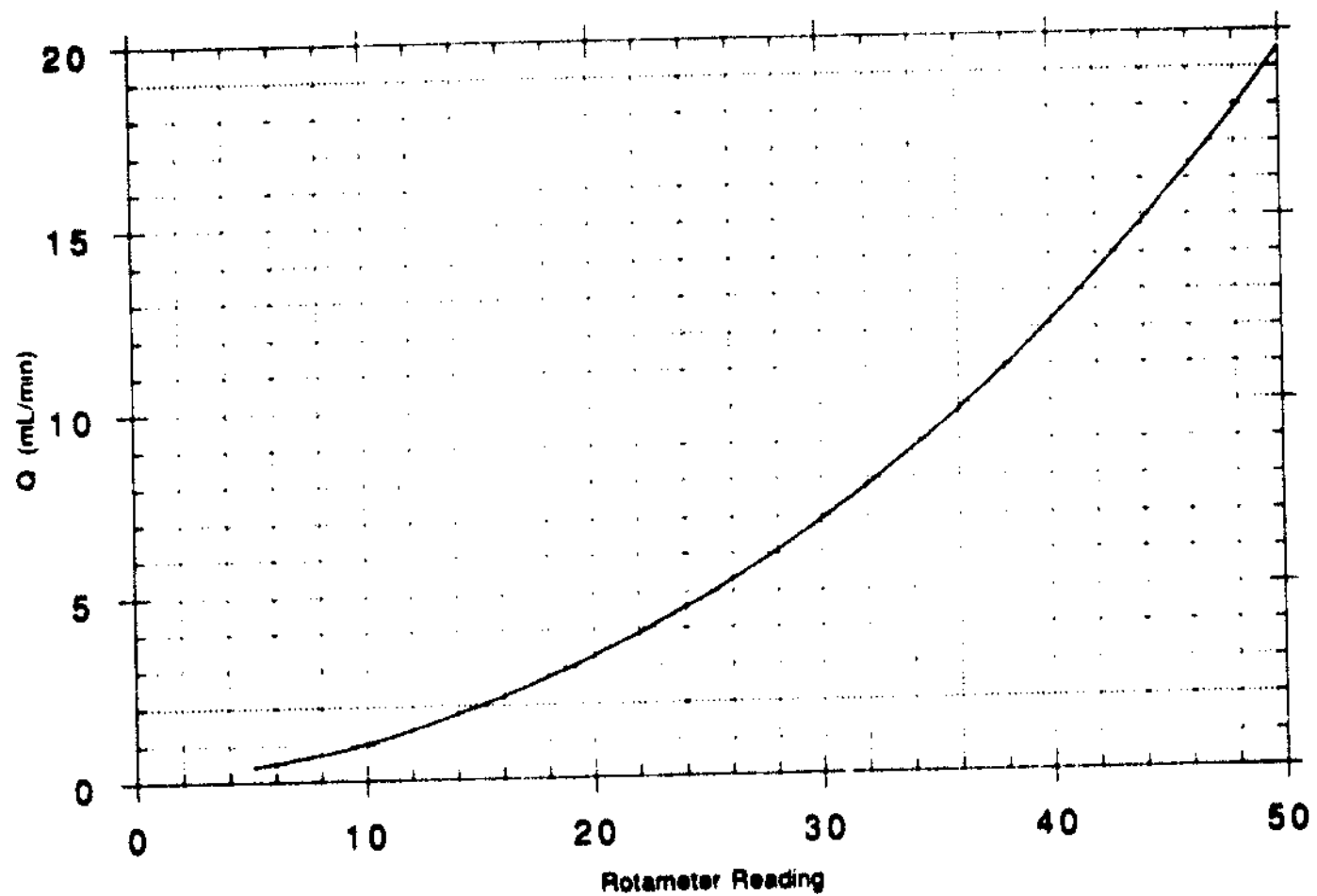
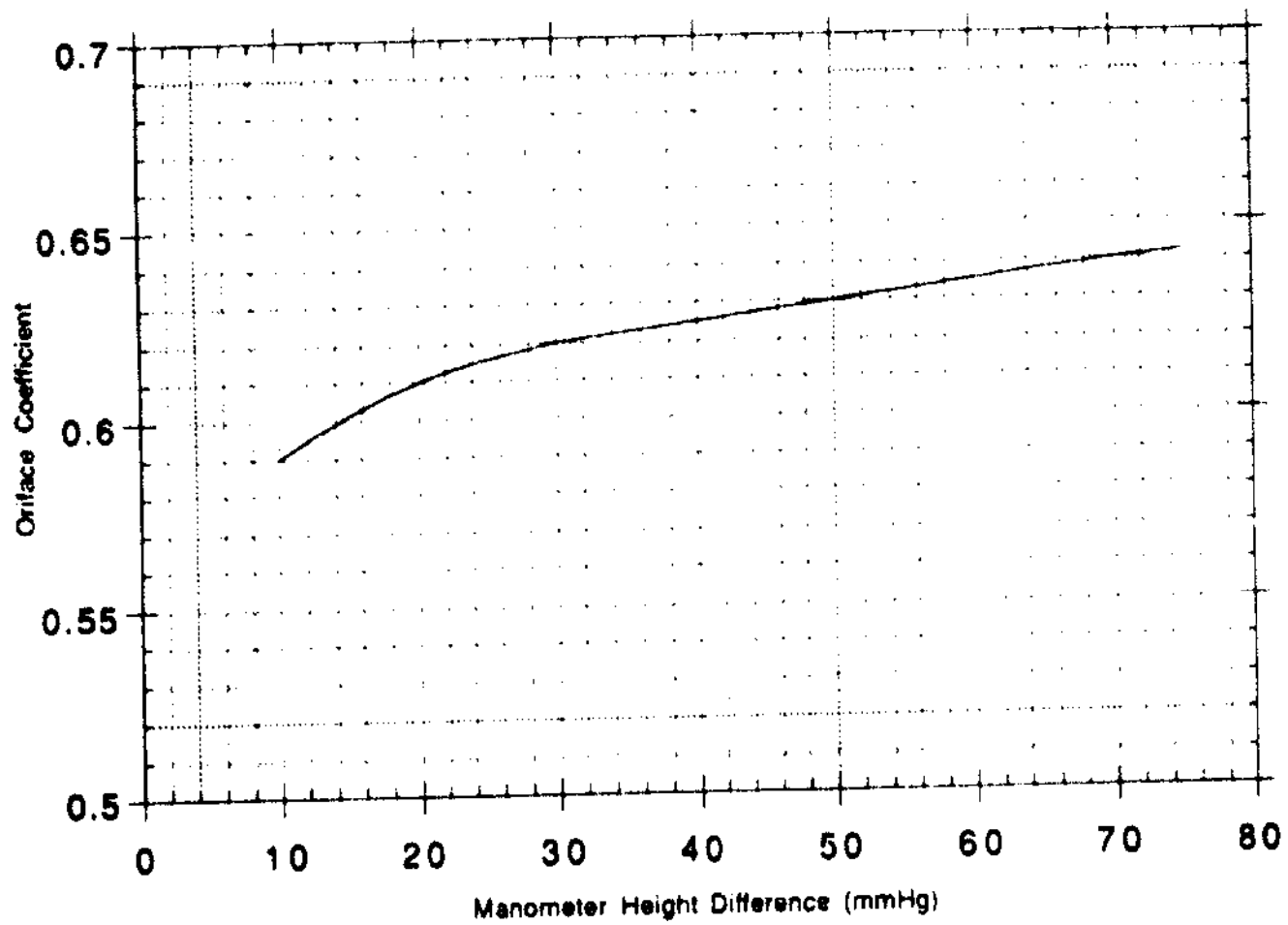


Figure B2: Orifice Coefficients for 0.524 in. Orifice Meter



## REFERENCES

1. Bennett, C. O. and J. E. Myers, Momentum, Heat, and Mass Transfer, 3rd edition, McGraw-Hill, 1982.
2. Laufer, J., "The Structure of Turbulence in Fully-Developed Pipe Flow," NACA rep. no. 1174, 1954.
3. Lee, M. M., "Droplet Motion and Deposition in Vertical Turbulent Pipe Flow," Ph. D. Thesis in Chem. Eng., University of Illinois, Champaign-Urbana, 1987.
4. Perry, R. H. (late ed.), Perry's Chemical Engineers' Handbook, 6th edition, McGraw-Hill, 1982.
5. Schmidt, D. A., "Droplet Dispersion in a Turbulent Vertical Flow," B. S. Thesis in Chem. Eng., University of Illinois, Champaign-Urbana, 1991.
6. Vames, J. S., "Droplet Dispersion in a Turbulent Pipe Flow," Ph. D. Thesis in Chem. Eng., University of Illinois, Champaign-Urbana, 1985.
7. Young, J. B. and T. J. Hanratty, "Optical Studies on the Turbulent Motion of Solid Particles in a Pipe Flow," J. Fluid Mech., 231, p.665-88, 1991.